

Humboldt-Universität zu Berlin

Department of Chemistry

*and*

Fritz Haber Institute of the Max Planck Society

Department of Physical Chemistry

electron dynamix - Stähler research group

## **Bachelor's thesis**

Out-Standing: Ultrafast dynamics of photogenerated  
monomers in a terrylene H-aggregate

submitted by: Johannes Lütgert

matriculation number: 589951

first assessor: Prof. Dr. Julia Stähler

second assessor: Prof. Dr. Emil List-Kratochvil

Berlin, 27.02.2021

# Contents

<b>1</b>	<b>Introduction</b>	<b>1</b>
<b>2</b>	<b>Fundamentals</b>	<b>3</b>
2.1	Electronic Properties of Molecules . . . . .	3
2.2	Organic Semiconductors and Crystals . . . . .	6
<b>3</b>	<b>Experimental Details</b>	<b>10</b>
3.1	Sample Preparation . . . . .	10
3.2	Static Absorption Measurement . . . . .	10
3.3	Static Photoluminescence and Time-correlated Single Photon Counting . . . . .	11
3.4	Transient Absorption Spectroscopy . . . . .	14
<b>4</b>	<b>Results</b>	<b>18</b>
4.1	Single Molecule – Textbook Molecule . . . . .	18
4.1.1	Static Electronic Properties . . . . .	19
4.1.2	Time-correlated Single Photon Counting . . . . .	21
4.1.3	Transient Absorption Spectroscopy and Electronic Dynamics . . . . .	23
4.2	Discussion of Single Molecule Behavior . . . . .	31
4.3	Thin Films of Terrylene . . . . .	33
4.3.1	H-Aggregate Formation in Thin Terrylene Films . . . . .	33
4.3.2	Induced Monomer Absorption . . . . .	35
4.3.3	Ultrafast Dynamics of Terrylene Films . . . . .	37
4.4	Discussion of Electronic Dynamics in Thin Terrylene Films . . . . .	44
<b>5</b>	<b>Outro</b>	<b>48</b>
	<b>References</b>	<b>50</b>
	<b>Appendix</b>	<b>51</b>



# 1 Introduction

All kinds of electronic devices and technologies have become an essential and indispensable part in all areas of our everyday life. A world without batteries, sensors, displays, computers and smartphones is not imaginable anymore. Nevertheless, future developments in the electronic and opto-electronic field are going to increase their possible applications and perhaps have the ability to change or shape the world in some areas of our life. The growth of the Internet of Things (IoT) and therefore the increasing number of powerful, connected and user-friendly devices will open the way for new opto-electronic applications, like advanced display technologies or photo-switchable components. Human responsibilities in the context of the climate change are going to increase the urgent need for environmentally friendly strategies for energy conversion and storage, like more efficient batteries and solar cells.

The development of advanced hybrid inorganic and organic systems (HIOS) allows to combine the advantages of organic and inorganic materials. For example, inorganic substances are magnificent regarding their electrochemical properties and their mechanical, chemical and thermal stability, while organic compounds convince with their synthetic flexibility and therefore widely adaptable characteristics, particularly concerning their optical, mechanical and microscopic properties. Modern approaches in the synthesis and fabrication of such hybrid devices enable scientists to design, build and control complex systems, in which different materials and their interactions are used to precisely tune the properties of the HIOS.<sup>[1]</sup> The great possibilities and chances of hybrid technologies lead to numerous research projects in different scientific fields. This thesis for example, was created as part of the Berlin-based collaborative research centre 951 "Hybrid Inorganic/Organic Systems for Opto-Electronics", which promotes a variety of interdisciplinary approaches to the development and research of hybrid devices.

Promising candidates for applications in light-harvesting or light-emitting are  $\pi$ -conjugated compounds, like the rylene family. They show strong absorbance and fluorescence in the UV-vis range, as well as a high chemical stability. The simple substitution of the aromatic backbone leads to highly adaptable properties of the rylenes, regarding their absorbance and emission wavelength, as well as their electron and hole transfer characteristics. Recent scientific works showed a variety of possible applications, such as light-emitting diodes, optical switches and photodetectors. Especially promising is the usage in organic photovoltaic (OPV) and organic field-effect transistors (OFET).<sup>[2]</sup>

To design and build such hybrid inorganic organic devices, a thorough understanding of the optical and electronic properties of the different components is necessary. In this thesis, terrylene, an unsubstituted member of the rylene family, is used to examine the ultrafast electronic properties of organic,  $\pi$ -conjugated chromophores. While most of the previous research in this field is centered around rylene-diimides, unsubstituted rylenes like terrylene did not get a lot of attention so far, especially regarding their ultrafast electronic properties.

The aim of these work is to estimate if terrylene is a promising material for such opto-electronic applications as described above. Therefore, the thesis can be divided into three major parts. First, revealing the basic electronic structure and the corresponding dynamics of single terrylene molecules in solution is a necessary foundation to understand the properties in the following steps. Because future applications will most likely contain terrylene or similar organic compounds in a solid state, we also want to understand how the electronic properties and dynamics change, when terrylene is applied in form of thin films, representing the surface properties of solid organic matrices. Finally, we want to answer the question if it is possible to change and manipulate the electronic states and dynamics in the film.

To reveal the static electronic properties of terrylene, static absorption and photoluminescence spectroscopy is applied. Besides that, time-correlated single photon counting as well as transient absorption spectroscopy are used to validate the static properties and to allow the investigation of the dynamics of the associated processes.

We found out that terrylene in solution behaves like a textbook molecule, showing strong absorption and fluorescence in the visible range with a long living excited state, which is especially promising for opto-electronic applications. In thin terrylene films, the interaction of molecules results in the formation of H-aggregates, characterized by a strong blueshift of the absorption bands as well as a complete fluorescence quenching. Compared to the single molecules, those films show more complex dynamics. For example, photoexcitation leads to a monomer-like absorption feature in the solid state. This is remarkable, because it shows the possibility of modifying the electronic properties on an ultrafast timescale. In addition to that, fit models are developed and applied to the transient absorption data of the single molecules and the film, both which are capable of describing the fairly complex behavior and revealing the underlying dynamics, by just using spectra from the static measurements and a noticeable small number of parameters.

The thesis starts with a brief overview about the necessary fundamentals in chapter 2, summarizing the basic electronic properties and processes of molecules, as well as the theory behind molecular crystals and aggregates. Chapter 3 explains the different experimental techniques used in this project, as well as the composition of the particular experimental setups. The results in chapter 4 start with the examination of the static properties of single terrylene molecules in solution (4.1.1), as well as their dynamics, which are revealed by time-correlated single photon counting (4.1.2) and transient absorption spectroscopy (4.1.3). Understanding the static properties and showing the formation of H-aggregates in terrylene films is done in chapter 4.3.1. A more extensive investigation of the dynamics is done in section 4.3.2 and 4.3.3 by evaluating and fitting the transient absorption data.

## 2 Fundamentals

### 2.1 Electronic Properties of Molecules

Molecules, as all quantum mechanical systems, can only exist in discrete states with distinct energy values. These states are called eigenstates, since they are eigenfunctions of the system's wavefunction. In the case of molecules, these states can be approximated by molecular orbitals, which are made from a linear combination of atomic orbitals. Nevertheless, a variety of effects can give rise to additional states or change their energy, for example the change of the excited state energy in molecular aggregates, as explained later. The lowest possible state of a molecule is called the ground state and is usually set to a reference energy of zero. Every other possible energy level above the ground state can be reached through excitation of the system and therefore they are called excited states. For example, the excitation of a molecule from the ground state to the first excited state could be described by the promotion of an electron from the HOMO to the LUMO.<sup>[3]</sup>

Especially interesting for spectroscopy is the interaction of matter with light, particularly how this interaction can change the energy state of the system. In the simplified model of a two-level system, as shown in Figure 1, a transition between two states can occur if a resonant electromagnetic wave is absorbed by the molecule. A wave is called resonant, if the photon energy  $h\nu$  of the light corresponds to the energy difference between the two states.

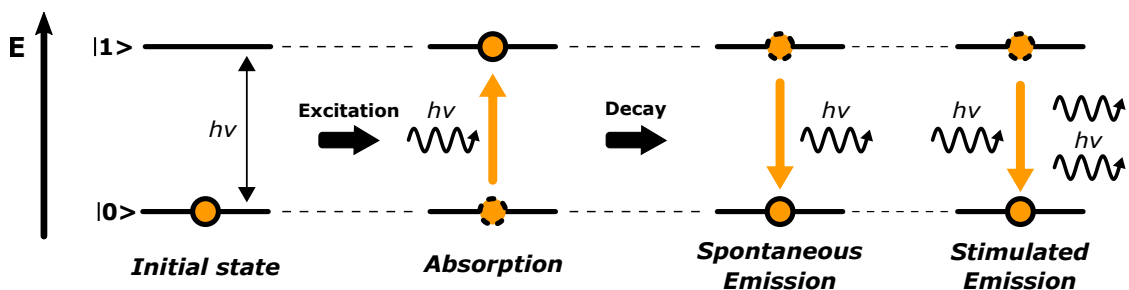


Figure 1: Radiative transitions in a two-level system.

After the system is excited into the higher state  $|1\rangle$ , there are two possible ways to relax into the ground state  $|0\rangle$ . Either by spontaneous emission of a photon, again with the same energy  $h\nu$  as the energy difference of the two levels, or by stimulated emission. Stimulated emission occurs if an excited molecule interacts with a resonant photon, leading to the emission of another coherent photon with exactly the same properties as the first photon.<sup>[3,4]</sup>

Unfortunately, this description is too simplified for a real molecule, which consists of a variety of states and different radiative and non-radiative transitions between them. An overview about the most important energy levels and transitions for a single molecule is given by the Jablonski-diagram in Figure 2.

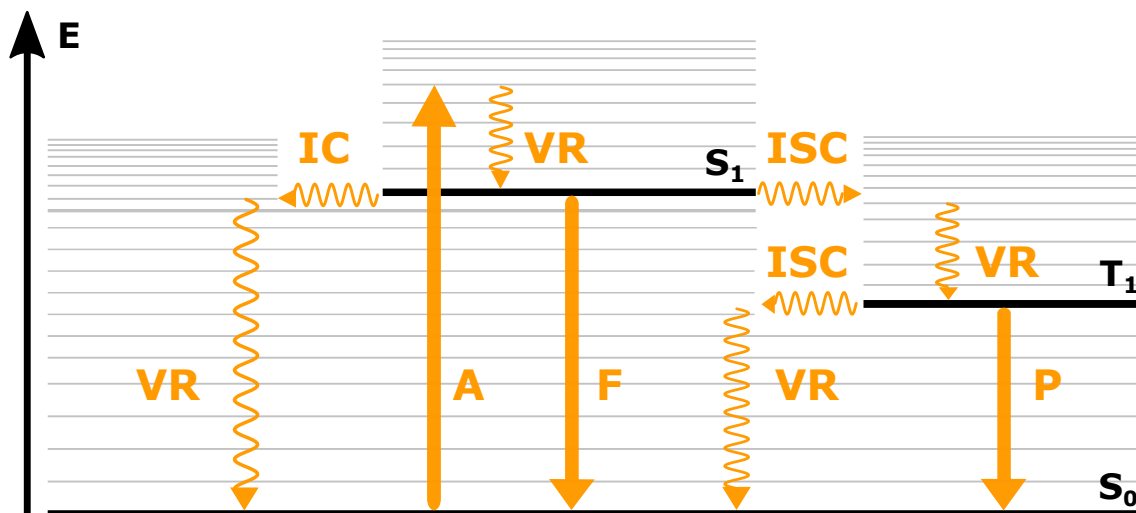


Figure 2: Jablonski-diagram, schematically showing different spectral processes in a molecule.

According to the Jablonski-diagram, a molecule consists of an electronic ground state  $S_0$  and different electronically excited states  $S_x$  and  $T_x$ , which stands for singlet and triplet states respectively. Additionally, every electronic state contains a variety of vibrational and rotational states. While electronically excited states usually have excitation energies of a few electronvolts, vibrational levels are only on the order of several millielectronvolts, while the rotational energy spacing is even lower and not shown in the Jablonski-diagram anymore.

As described earlier, absorption (A) of light leads to the population of electronically and vibrationally excited states. From there on, the molecule can relax to the ground state on different ways. Fast vibrational relaxation (VR) leads to the non-radiative decay into lower vibrational levels of the same electronic state, mainly due to collisions with surrounding molecules. After this, the molecule can either change into a lower electronic state with the same spin-multiplicity by internal conversion (IC), from where vibrational relaxation (VR) to the ground state can occur, or it can undergo fluorescence (F). Fluorescence is a form of spontaneous emission, where the energy loss is accomplished by emitting a photon of the desired wavelength. Fluorescence can only occur between states of the same spin multiplicity, mostly between two singlet states. Therefore, it is spin-allowed and thus has a short lifetime. Due to intersystem crossing (ISC) it is also possible for the molecule to change from an excited singlet state to a triplet state. The triplet state itself will relax into its lowest vibrational level and then change to the singlet ground state either by intersystem crossing (ISC) or phosphorescence (P). Phosphorescence is another form of spontaneous emission, but between two states with different spin-multiplicity. Hence it is spin-forbidden, which results in a long lifetime of the triplet state.<sup>[3,5]</sup>

As already indicated in the Jablonski-diagram, transitions are not only possible between electronic states, but also between their different vibrational states. According to the Born-Oppenheimer-approximation, the electrons and nuclei have such a great difference in their masses that they move on different timescales. An electronic transition happens in roughly  $10^{-15}$  s, while a vibration of the nuclei needs  $10^{-13}$  s. From the perspective of an electron, the nuclei does not change its position during an electronic transitions. On the other hand, the nuclei is surrounded by an average distribution of the electrons. Hence it is feasible to neglect the interaction between electronic and vibrational transitions for most molecules. Only strongly vibronic coupled systems cannot be approximated by this theory.<sup>[4,5]</sup>

Based on this, the Franck-Condon principle is capable of describing the position and line shape of absorption and emission spectra, as illustrated in Figure 3. Therefor the ground and excited state  $S_0$  and  $S_1$  are represented by anharmonic potentials, which contain the wavefunctions (illustrated in yellow) of their different vibrational states  $\nu$ . An excitation can now be described as a vertical line according to the Born-Oppenheimer-approximation, because the nuclei will not change their distance in the short time of the electronic transition. Because the amplitude of a transition depends on the overlap of the wavefunctions of the initial and final state, the Franck-Condon principle allows to predict the intensity of such transitions, based on the overlap of two vibronic wavefunctions. The strongest transition for the example molecule in Figure 3 is shown as a blue arrow.

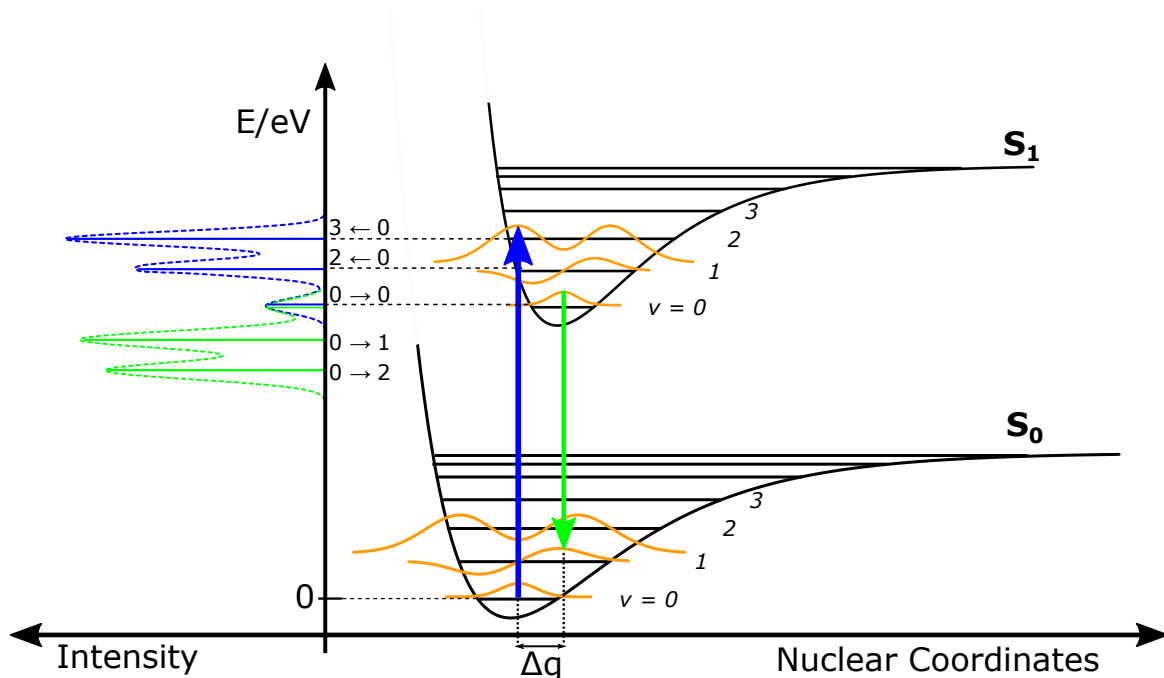


Figure 3: Visualization of the Franck-Condon principle, containing the major transitions of absorption (blue) and emission (green) between the ground state  $S_0$  and excited state  $S_1$ , as well as the corresponding spectra.

Besides the absorption spectrum, the Franck-Condon principle can also describe the emission spectrum in a similar way. The difference is, that according to Kasha's rule, the system will undergo a fast non-radiative decay into the lowest vibrational level of the excited state until the emission takes place. This loss in energy results in a redshift of the emission spectrum, which is called the Stokes-shift.

The aim of every physical system to minimize its energy results in the decay of excited states. Depending on the stability of such a state, different lifetimes can occur. The decay of an excited state can be described by a sum of exponential decay functions, one for every process that contributes to the overall decay, for example one for the vibrational relaxation and one for the subsequent fluorescent transition. Hence the decay function has the following form:

$$I(t) = \sum_i e^{\frac{-t}{\tau_i}} \quad (1)$$

where  $I(t)$  is an arbitrary intensity for the transition from the excited state, depending on the spectroscopy method applied, and  $\tau$  is called the exponential decay constant. Mathematically,  $\tau$  is the time, at which the population of the excited state is reduced to  $1/e$ , usually called the lifetime of this state. If all spectral processes can be distinguished by a separate exponential function, the corresponding lifetimes refer to only one of these processes, otherwise it is just an average lifetime.<sup>[5]</sup>

## 2.2 Organic Semiconductors and Crystals

The term of organic semiconductors refers to a class of molecules, which combine the advantages of organic compounds and classic semiconductors. This is on the one hand the strong absorption and sometimes strong photoluminescence in the UV-Vis region, as well as the ability to conduct electricity. On the other hand, the chemistry behind organic molecules is widely studied and understood, allowing to easily synthesize and modify a variety of organic compounds, to change and adjust the properties needed for certain applications. This applies not only for the opto-electronic properties stated above, but particularly for their material structure. For example, they often show good solubility, but also they allow the fabrication of mechanically robust, but flexible films. In contrast to classical semiconductors they have a much higher bandgap, usually around 2 – 3 eV, so that thermal occupation of excited states and thus the occupation of charge carriers is not possible. Therefore, the electronic behavior is mainly dominated by optical excitations and processes, leading to applications especially in the field of opto-electronic devices like organic solar cells or light emitting diodes.<sup>[4]</sup>

In the following chapter, the important organic semiconductor class of rylenes and the investigated molecule terrylene are briefly reviewed, followed by an overview about the electronic and optical properties of molecular crystals, which are predominant for organic chromophores in the solid state.

## Rylene-family and Terrylene

The “rylene-family” is a class of organic chromophores and semiconductors, which consist of different numbers of condensed naphthalene units, as shown in Figure 4. Especially interesting for this thesis is the terrylene molecule, which contains four naphthalene units.

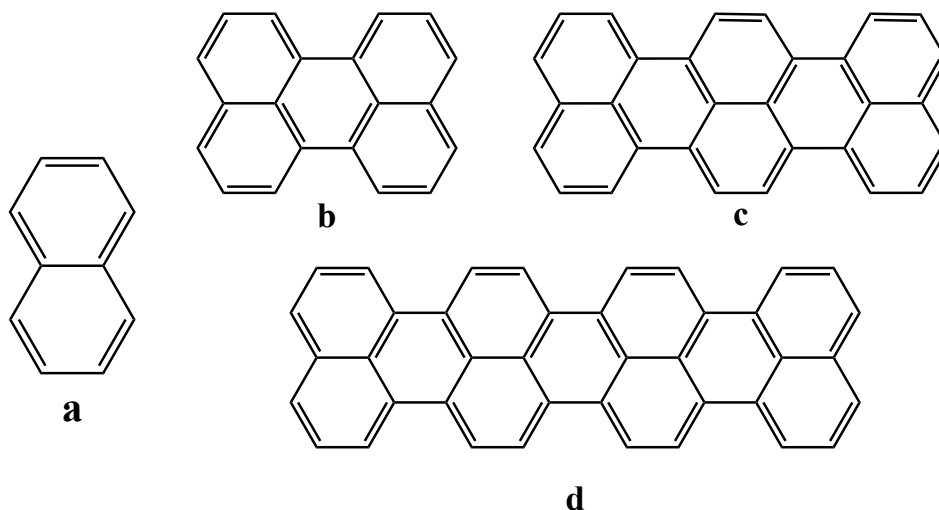


Figure 4: Naphthalene (a), Perylene (b), Terrylene (c) and Quaterrylene (d).

Rylenes have a variety of properties, which make them promising candidates for electronic applications like organic solar cells, dye lasers and organic field effect transistors <sup>[1]</sup>, as well as for the investigations of biological systems with rylene-based fluorescent dyes. They show strong absorption in the UV-Vis region, an exceptional high fluorescence quantum yield and an excellent photophysical and photochemical stability. Because of their extended and polarizable electron system, they tend to aggregate under strong fluorescence quenching. Through their low solubility in non-organic solvents, they already show aggregation for example in water.<sup>[6]</sup>

The electronic behavior of these molecules and their interaction with light is mainly determined by their conjugated  $\pi$ -electron system, because it makes up the HOMO orbital. All carbon atoms are connected through single  $\sigma$ -bonds. Additionally, every atom can form a double bond to one other carbon atom, which is called a  $\pi$ -bond. In a conjugated system, the electrons that are occupying this  $\pi$ -bonds are delocalized, meaning that they are spread over the whole molecule.

The absorption of light leads to a transition from the HOMO to the LUMO, which consists of anti-binding  $\pi^*$ -orbitals. The resonance energy for this transition strongly depends on the size of the conjugated system and the chemical environment, especially the substitution of the aromatic system.<sup>[7]</sup> For unsubstituted rylenes, the absorption wavelength is mostly in the UV-Vis region. While the absorption of perylene lies below 600 nm, terrylene already absorbs at a wavelength of 550 nm.<sup>[6]</sup>

Aromatic compounds are an easy target for a variety of organic reactions, which allows to introduce different functional groups into the rylene-framework. The most popular derivatives are the rylene-diimides (RDI), which contain two imide groups. All kinds of properties can be modified by the introduction of suitable functional groups. For example, the solubility in polar solvents like water can be increased by the substitution with polar groups, like sulfonyl groups, and the absorption band can be tuned in a wide range by using electron-pulling or -pushing groups.<sup>[6]</sup>

### Theory of Aggregation and Molecular Crystals

Ideal molecular crystals are made out of perfectly ordered and aligned molecules, especially flat aromatic compounds, such as the rylene-family. In comparison to classic crystals, in which the components are interacting due to strong covalent or ionic bonds, organic molecular crystals are held together by weak van-der-Waals (vdW) interactions. They result from an attractive force between molecules, which have temporary dipole moments. These dipole moments can arise from fluctuations in the charge distribution and induce dipole moments in adjacent molecules, even if those molecules are non-polar. The strength of vdW-forces strongly depends on the distance between two neighboring molecules and their polarizability, which is the ability for charge redistribution. As discussed above, rylenes like terylene have large, delocalized  $\pi$ -electron systems, which results in a high polarizability and hence the possibility to develop strong vdW-forces in dense crystal arrangements, like the herringbone structure.<sup>[4]</sup>

Excitations in semiconducting or insulating materials result in bound electron-hole pairs that can be described as quasi-particles, called excitons. The attractive Coulomb-force between the negatively charged electron and the positive hole reduces the resonance energy of the exciton compared to the excitation energy in an unbound case. Mott-Wannier excitons are electron-hole pairs with a large distance, while in Frenkel-excitons the pair is localized near one lattice site. Organic semiconductors usually have absorption energies in the range of 2 – 3 eV and hence the thermal occupation of excited states is neglectable. This fact and the low dielectric constant of about  $\epsilon_r = 3.5$ , leads to a significant Coulomb interaction between electrons and holes. Consequently, electronic excitations in molecular crystals can be described as Frenkel-excitons that are localized on one molecule or lattice site.<sup>[4,5]</sup>

The interaction of molecules in a molecular crystal and the consequences for their electronic behavior can often be described by a simple model of two strongly coupled monomers, forming a dimer. An accurate description of this interaction requires to take into account the Coulomb interaction between the whole electron densities of both molecules. Calculating the electronic distribution of the monomers and subsequently determine their interaction is laborious. That is why Kasha developed a simplified model, in which these interactions are approximated by dipole-dipole interactions between the transition dipole moments of the monomer units.

According to Kasha, the aggregation and hence the interaction of the transition dipole moments has two important consequences for the energy states of the molecules, as seen in Figure 5. First, the energies of the ground state and excited state are lowered by the gas-to-crystal shift, which mainly arises due to dispersion effects. Secondly, the excitons of the monomer units interact, forming two new exciton states, called  $E'$  and  $E''$ . In the field of molecular crystals, this energy difference is usually referred to as the Davydov-splitting  $2\beta$ . The population of these two states and hence the electronic properties of the dimer depend on the alignment of the transition dipole moments of the monomers. Two extreme cases can be formulated: If the transition dipole moments are parallel, only the transition to the higher lying exciton state  $E''$  are dipole-allowed, resulting in a blueshift of the absorption energy. Because of this Hypsochromic shift, these types of aggregates are called H-aggregates. Transitions to the lower energy state  $E'$  are only allowed for a head-to-tail arrangement of the transition dipole moments, which is the case for a J-aggregate. In contrast to these extreme cases, an oblique arrangement of monomers will result in the population of both states.

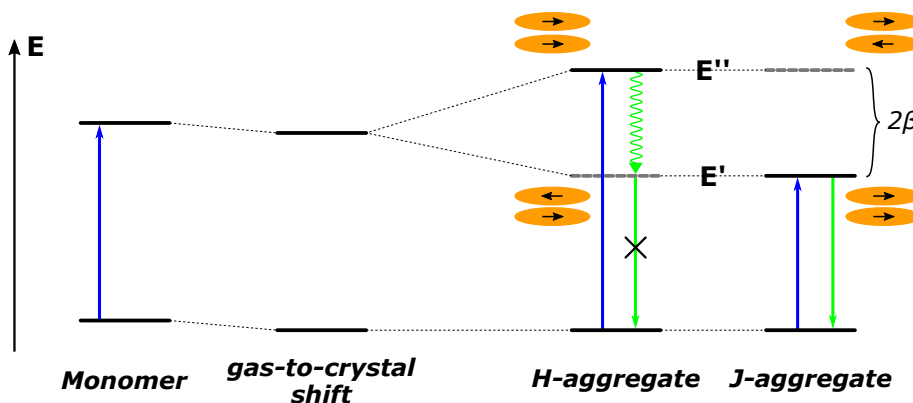


Figure 5: Schematic representation of electronic states in a monomer and in aggregates, as well as associated electronic transitions.

The formation of these two types of aggregates shows great impact on the optical properties of the original material. As mentioned above, the absorption in H-aggregates is blue-shifted, while in J-aggregates absorption and emission are red-shifted. According to Kasha's rule, molecules relax into their lowest excited state due to fast vibrational relaxation before emission processes can occur. Consequently, H-aggregates relax to the  $E'$ -state very quickly. Because the transition between the ground state and the  $E'$ -state is dipole-forbidden in H-aggregates, as explained before, this state shows no photoluminescence and decays due to non-radiative pathways.<sup>[8,9]</sup> It is important to mention and understand, that the excitation of an aggregate no longer corresponds to the excitation of one monomer unit, rather it is delocalized over the aggregate and can be quantum mechanically described as a linear combination of the excitons of the monomer units. If one moves further to aggregates with more than two monomers, or even to molecular crystals with a tremendous number of molecules, the number of exciton states will increase, forming a band-like structure in which the exciton is further delocalized across a wide range.<sup>[8]</sup>

### 3 Experimental Details

The following chapter is about the experimental techniques that were used for this thesis. For every method, a brief overview about the mechanism is given, as well as the actual experimental setup and the specifications for the performed measurements. The chapter starts with details about the samples, then moves on to the static absorption and photoluminescence measurements and finishes with an overview about time-correlated single photon counting and transient absorption spectroscopy.

#### 3.1 Sample Preparation

In this thesis, the aim is to investigate the electronic behavior of terrylene in solution and in the solid state. Therefore, samples of terrylene in both forms are needed. Terrylene itself was synthesized and provided by the HechtLab at the Humboldt-Universität zu Berlin.

As a solvent for the liquid samples *para*-xylene is used. The solid terrylene is dissolved in *para*-xylene to yield a stock solution with a concentration of 4  $\mu\text{M}$ . Sample 1 (**S1**) consists of only the stock solution in a cuvette, while Sample 2 (**S2**) is diluted with *para*-xylene to a concentration of 1  $\mu\text{M}$ .

For the film sample, a fused silica plate was cleaned in an ultra-high vacuum chamber and then coated with terrylene using a Knudsen cell. The system was calibrated using a quartz crystal microbalance to allow for a reproducible layer thickness. The sample used in this thesis has a layer thickness of approximately 50 – 60 nm.

#### 3.2 Static Absorption Measurement

Static absorption measurements, usually referred to as UV-Vis spectroscopy, are used to investigate the absorption of molecules in the ground state. A light source with a broad spectrum is used to illuminate the sample. Photons with an energy that corresponds to the resonance energy of an electronic transition will be absorbed and hence the intensity of the transmitted light will decrease at this specific wavelength. According to Beer-Lambert's law, the intensity decrease in an infinitesimal thin layer of the sample  $dd$  is proportional to the extinction coefficient  $\epsilon^*$  and the sample concentration  $c$ . Integrating this equation for a real sample thickness  $d$  and converting the natural logarithm to an decimal logarithm, results in the following logarithmic relationship between the measured intensities and the absorbance  $A$ :

$$dI_1 = -I_0 c \epsilon^* dd \quad \Rightarrow \quad A(\lambda) = c \epsilon d = -\log \left( \frac{I(\lambda)}{I_0(\lambda)} \right) \quad (2)$$

where  $I(\lambda)$  is the intensity of the transmitted light and  $I_0(\lambda)$  is the intensity of the light source, used as a reference. By using a monochromator, the detector determines the intensities separately for every wavelength, resulting in the absorption spectrum of the sample.

The samples of terylene in solution are measured using an *Agilent Cary 50* spectrometer, in a spectral region between 1.55 and 3.54 eV. To be able to measure the full absorption spectrum of the solid samples in the far UV region, measurements of the film are performed with a *PerkinElmer Lambda 950* spectrometer for photon energies between 1.46 eV and 6.89 eV.

### 3.3 Static Photoluminescence and Time-correlated Single Photon Counting

#### Laser System

For the following photoluminescence measurements, a *Coherent* femtosecond laser system, schematically shown in Figure 6, is used. A pulsed Titanium:Sapphire laser (Ti:Sa), *Vitara*, provides fundamental pulses at 1.55 eV with a repetition rate of 200 kHz. To prevent damaging the optical medium in the regenerative amplifier, the pulses are first stretched in time to reduce their peak intensity. The regenerative amplifier *RegA 9000* is then used to amplify the pulses. For this purpose, one single pulse is coupled into a Ti:Sa-crystal, which is pumped by a continuous wave laser *Verdi* with a photon energy of 2.32 eV. After multiple cycles in the crystal, the amplified pulse is coupled out. After recompression of the pulses, the system offers laser light with a photon energy of 1.55 eV, a power of 1.8 W and a pulse duration of around 40 fs.

This beam can either be directly used or it is sent into an optical parametric amplifier *OPA*, which allows to adjust the wavelength in a broad range. To achieve this, the beam is split into two parts. One is used to generate a white-light continuum using a sapphire crystal, which seeds a non-linear BBO crystal. In addition, this crystal is pumped by the second beam. Depending on the alignment of both beams, a narrow band of the white-light continuum is selected and amplified in the BBO-crystal. Right after the *OPA*, a prism compressor further reduces the pulse duration. For the performed measurements in this thesis, the *OPA* is adjusted to a photon energy of 2.5 eV, yielding an output power of approximately 23.4 mW.

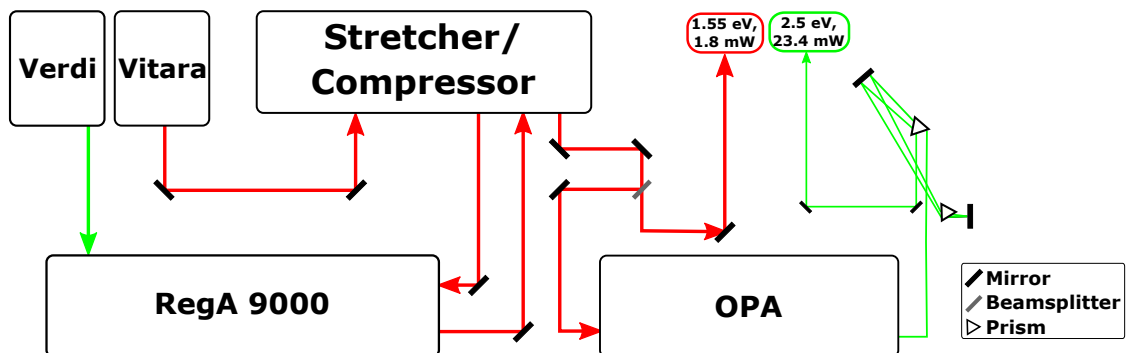


Figure 6: Schematic drawing of the RegA-laser system.

## Static Photoluminescence Spectroscopy

The setup used to measure static photoluminescence spectra of the terrylene samples is shown in Figure 7. A pulsed laser beam from the *RegA*-system with a photon energy of 2.5 eV and a maximum power of 23.4 mW is used to pump the sample. With a continuously variable neutral density filter, the power is reduced to different values, which allows the investigation of possible fluence-dependent properties. For the terrylene samples, beam powers between 50  $\mu$ W and 2 mW are used. The beam is focused onto the sample cuvette with a lens, resulting in a beam diameter of approximately 100  $\mu$ m at the sample position. The pump beam excites molecules in the sample, which then undergo emission in all spatial directions. For this reason, two parabolic mirrors and a lens are used to collect and focus as much of the emitted light as possible. After passing an optical high-pass filter with a cutoff energy of 2.36 eV, to remove residual light from the pump beam, the emission light is directed into an optical fiber. At the end of the fiber, the photoluminescence spectrum is recorded using an *Andor Technology Shamrock SR303i* spectrometer, which provides a spectral resolution of approximately 0.1 nm.

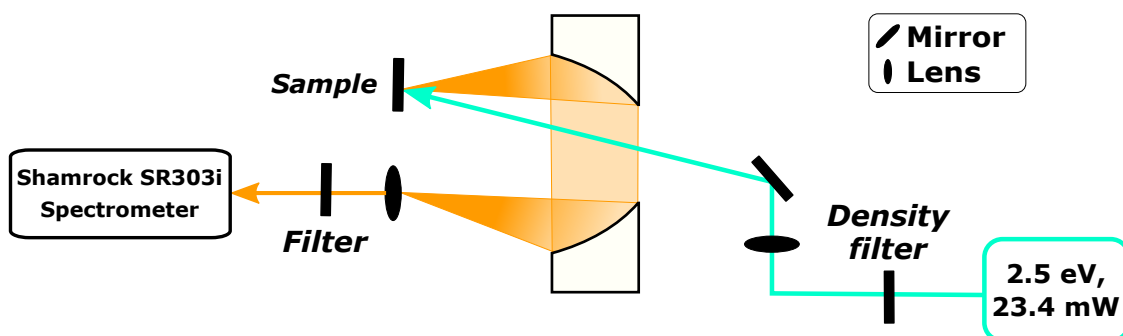


Figure 7: Schematic drawing of the static photoluminescence spectroscopy setup.

## Time-correlated Single Photon Counting

Time-correlated single photon counting can be used to investigate emission processes of molecules, especially measuring the decay mechanisms and corresponding lifetimes. A TCSPC setup consists of a pulsed laser source, which repeatedly excites the sample, and a detector, which is capable of detecting single photons. To measure a TCSPC trace, a very low detection rate is needed, usually only one photon per hundred excitation pulses, so that the detection of multiple photons in one measurement cycle is extremely unlikely. Repeatedly measuring the time between the excitation of the sample and the detection of an emitted photon results in a histogram containing the individual lifetimes. After a sufficient number of repetitions, this histogram reflects the exponential decay curve of the emission process, which allows the determination of the lifetime of the underlying electronically excited state.<sup>[10]</sup>

The experimental setup again uses a pulsed laser beam from the *RegA*-system, with a photon energy of 2.5 eV and a maximum power of 23.4 mW. Using a beam splitter, the beam is divided into two parts. One is going to a fast photodiode, which works as a trigger to start the measurement timer. The second part of the beam is used to excite the sample. To allow the measurement at different pump powers and to assure a low detection rate, the beam power can be adjusted using a continuously variable neutral density filter. For this thesis, the terrylene samples are measured at beam powers between 50  $\mu$ W and 2 mW. The beam is then focused onto the sample, where it causes fluorescence. The emitted light is focused and directed into the *Bentham TMc150* monochromator, which allows to select only a narrow band, in which the emission is to be investigated. An additional high-pass filter at 2.36 eV removes residual light from the pump beam, to protect the sensitive detector and to assure, that only photons from the emission process are measured. The following *PicoQuant PMA Hybrid 06* photomultiplier detector is then able to detect a single photon, which stops the measurement timer. Using a suitable acquisition software, a large number of cycles are measured to yield a histogram of the emission process.

The resulting decay curve is convoluted with a so-called instrument response function (IRF). This function includes the temporal resolution of the detector and acquisition system, which broadens up the curve, as well as it takes the time delay between the triggering of the photodiode and the arrival time of the pump pulse at the sample into account.

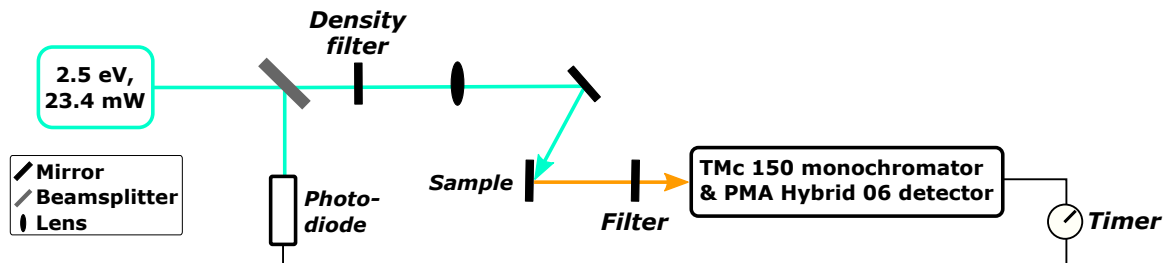


Figure 8: Schematic drawing of the TCSPC-setup.

### 3.4 Transient Absorption Spectroscopy

#### Mechanism

Transient absorption spectroscopy is a powerful pump-probe measurement technique, which allows to investigate the time-dependent electronic properties of matter. The basic principle behind pump-probe measurements is illustrated in Figure 9. For that, two different pulsed laser beams are used. The first strong beam, called the pump, has a narrow linewidth and excites the sample at a specific energy. The weak probe beam consists of broadband white-light laser pulses, which are used to measure the absorbance of the sample over a broad spectral region. Measuring the absorbance with and without the pump then yields a differential absorbance spectrum between the molecules in an excited state and in the ground state. To assure that a sufficiently large fraction of probed molecules is in the excited state, the pump beam needs to be much more intense than the probe beam, usually on the order of tens or hundreds of times more. By varying the delay between the two pulses, this differential absorbance can be measured at different times after the excitation. While other time-dependent measurement techniques only allow to measure the time at which a specific event happens, in the case of TCSPC the emission of a photon, the advantage of pump-probe experiments is that they are capable of investigating the systems properties at any time after the excitation.

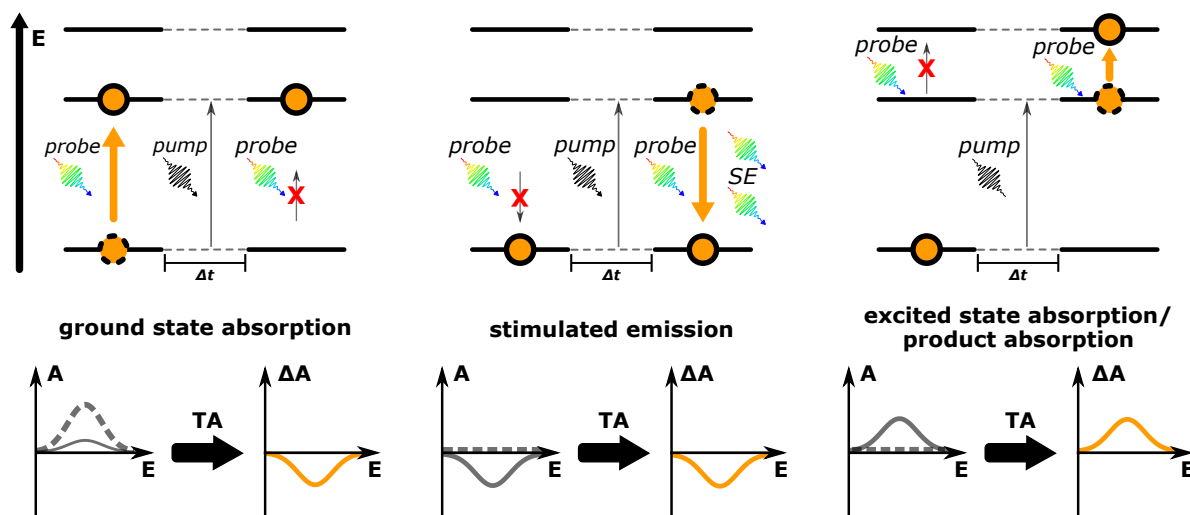


Figure 9: Top: Pump-probe mechanism for different spectral features. Bottom: Absorbance with (gray, solid) and without (gray, dashed) pump, as well as the resulting TA signal (yellow).

In TA spectroscopy, the resulting signal is a differential absorbance and hence depends on the different absorption behavior in the ground state and in an excited state. According to that, the transient absorption signal  $\Delta A(\lambda, t)$  for every pump-probe delay  $t$  is given by the following equation:

$$\Delta A(\lambda, t) = A_e(\lambda, t) - A_{gs}(\lambda) = -\log \left( \frac{I_e(\lambda, t)}{I_{gs}(\lambda)} \right) \quad (3)$$

where  $A_e(\lambda, t)$ ,  $I_e(\lambda, t)$  and  $A_{gs}(\lambda)$ ,  $I_{gs}(\lambda)$  are the absorbances  $A$  and measured intensities  $I$  at the specific time delay  $t$  for an excited state (e) and the ground state (gs), and thus with and without the pump respectively. The differential absorbance  $\Delta A(\lambda, t)$  is usually given in the units of optical density  $OD$  or  $mOD$ .

Depending on the different absorption behavior in the ground state as well as in the excited state, different spectral processes show a varying differential absorbance, which allows to distinguish them by their signal in a transient absorption spectrum. The most prominent spectral features which can occur in TA spectra are shown in Figure 9 and are further discussed in the following paragraphs:

- Absorption from molecules in the ground state produces a positive signal  $A_{gs}$  in the unpumped sample. After the excitation, there are fewer molecules in the ground state and therefore the absorbance  $A_e$  is smaller than the unpumped absorbance. This results in a *negative* TA signal, which is called *ground state bleach* (GSB). Because the GSB signal is determined by the ground state absorption, it reflects the line shape and spectral position of the static absorption spectrum.
- Excited molecules can absorb a second photon, leading to a transition to a higher excited state, called *excited state absorption* (ESA). Because this is only possible for excited molecules, the absorption  $A_{gs}$  in the unpumped sample is zero, while the absorption  $A_e$  in the excited sample is positive, leading to a *positive* signal in the TA spectrum.
- An excited molecule can also decay through *stimulated emission* (SE). During the stimulated emission, one incident photon induces the emission of a second, coherent photon with the exact same properties as the first one. Consequently, the number of photons at the detector increases in the excited state, yielding a negative absorption  $A_e$ . Because stimulated emission can only occur from an excited state, the corresponding absorption  $A_{gs}$  without the pump pulse is zero, thus the resulting TA signal is *negative*. Stimulated emission shows the same spectral position as spontaneous emission, for example measured by static fluorescence spectroscopy. As well as the photoluminescence, it is Stokes-shifted regarding the ground state bleach.

- Beside these most important features, other spectral processes can occur and will result either in a positive or negative differential absorbance. Most prominent is the term “*Absorption by product*” or “*Product absorption*”, which generally stands for absorption processes of all kinds of photoexcited species, like intermediate products of photochemical reactions. Because it will only cause absorption in the pumped and hence excited state, it always gives a *positive* signal.

In real TA measurements, these features often overlap, which complicates their distinction and interpretation. Nevertheless, TA spectra contain information on the type of spectral processes, the spectral position of these, as well as their dynamics and temporal evolution, making it a useful tool for studying the static and ultrafast properties of all kinds of photophysical and photochemical processes. Especially important is the ability to measure the behavior of excited species, for example dark states, which are usually not observable with static spectroscopy.<sup>[11,12]</sup>

### Experimental Setup

For measuring the transient absorption spectra of terrylene in solution and as a film, the experimental setup schematically shown in Figure 10 is used.

A *Femtolasers sPro* Ti:Sa-laser generates 30 fs fundamental pulses with a photon energy of 1.5 eV. The fundamental beam is split into two parts, one for the pump with a pulse energy of 0.6  $\mu$ J, and one for the probe beam, with a pulse energy of 20  $\mu$ J respectively. The laser system provides a repetition rate of 1 kHz, which is halved by chopping every second pulse.

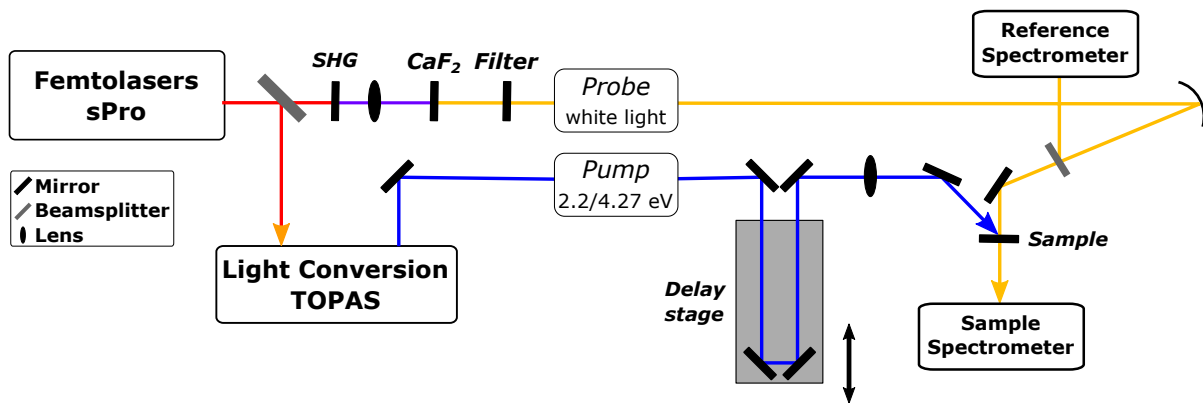


Figure 10: Schematic drawing of the transient absorption setup.

The photon energy of the pump beam can be changed to 3 eV or 4.6 eV, through second or third-harmonic generation in non-linear crystals. An optical parametric amplifier (*Light Conversion TOPAS*) is then used to adjust the photon energy of the beam to the desired pump wavelength. The beam then goes to a delay stage, which controls the pump-probe delay by variation of the beam path length, before it is focused with a lens onto the sample. The measurements of the terrylene samples are performed using pump pulses with an energy of 160 nJ

and 600 nJ to account for non-linear effects. For investigating terrylene in solution, a pump photon energy of 2.2 eV is used, while the film measurements are accomplished at a photon energy of 4.27 eV. The pump beam has a diameter of around 100 – 200  $\mu\text{m}$  and intersects with a small angle of  $5^\circ$  with the probe beam on the sample to prevent disturbances of the pump pulses in the spectrographs.

To generate the white-light continuum probe pulses, the beam is frequency-doubled first, before it is focused just before a 1 mm  $\text{CaF}_2$ -plate. Subsequently, a fused silica cuvette filled with a mixture of different dyes is used as a filter to spectrally flatten the continuum pulses. Monitoring of these continuum probe pulses is necessary to calculate the resulting signal. For this, a 50:50 beam splitter is used, splitting the probe beam into a reference and a sample beam. The resulting probe beam at the sample has a pulse energy below 0.1  $\mu\text{J}$  and a diameter of approximately 80 – 100  $\mu\text{m}$ . The sample absorption is measured in a range from 1.35 to 2.5 eV for terrylene in solution, and between 1.2 and 4.5 eV for the film sample.

Measuring the spectrum of the reference and sample beam is done by two home-made spectrographs. They consist of multiple gratings, arranged in a Czerny-Turner setup, to disperse the spectrum, which is then recorded with photodiode arrays. Transient absorption spectra are measured with different step sizes for the pump-probe delay, respectively 20 fs, 400 fs and 8 ps. The acquisition software automatically calculates the differential absorption signal, averages it over multiple pump-probe scans and corrects the signal for the chirp of the probe pulse as well as the background signal. With this setup, an instrument response of 0.1 ps and a timing precision of 0.02 ps can be achieved.<sup>[13,14,15]</sup>

## 4 Results

The investigation of the electronic properties and dynamics of thin terrylene films shows a fairly complex behavior, including different electronic processes like aggregation and induced monomer formation, which occur with different rise and decay times. To be able to properly understand and describe these features, it is necessary to first understand the properties of single molecules of terrylene. In chapter 4.1, the behavior of single molecules is examined, paying attention to the static spectral properties in 4.1.1 and the dynamics of this system in 4.1.2 and 4.1.3, revealing that terrylene in solution can be called a textbook-like molecule, showing strong absorption and photoluminescence in the visible range with a fairly long lifetime of 4 ns. Subsequently the static properties of thin terrylene films are described in chapter 4.3.1, especially the formation of H-aggregates which leads to a blue-shift of the absorption spectrum. Finally the dynamics of solid terrylene are discussed in section 4.3.2 and 4.3.3, especially revealing the formation of induced monomer.

### 4.1 Single Molecule – Textbook Molecule

In the following chapters, the properties of terrylene as a single molecule in *para*-xylene solution are investigated using static and time-resolved measurement techniques. In section 4.1.1, static absorption and photoluminescence spectroscopy reveal a textbook-like absorption and emission spectrum, showing absorption with a maximum at 2.21 eV and Stokes-shifted fluorescence at 2.03 eV. By using time-correlated single photon counting in chapter 4.1.2, a fairly long lifetime of 4 ns can be obtained for the excited state. Finally in section 4.1.3, a fit model for the transient absorption data is introduced, allowing to explain the different spectral processes involved, as well as extracting their dynamics.

For the development of complex applications, for example HIOS devices, a strong understanding of the separate materials and their interaction is necessary. Thus, a molecule like terrylene, which shows a simple behavior with predictable, textbook-like properties is favored. The long lifetime of the excited state is another advantage, especially to increase the chances for energy or charge transfer.

### 4.1.1 Static Electronic Properties

The fundamental electronic processes of a molecule are the absorption and emission of photons, leading to transitions between different electronic states, especially between the ground and first electronically excited state. To obtain information about those processes, static absorption and photoluminescence spectroscopy were conducted. The resulting static absorption and emission spectra are shown in Graph 11. The spectra are both normalized to one, to account for the different intensities that emerge from the differences in the spectroscopical methods, to allow for a far better comparison of the spectral features.

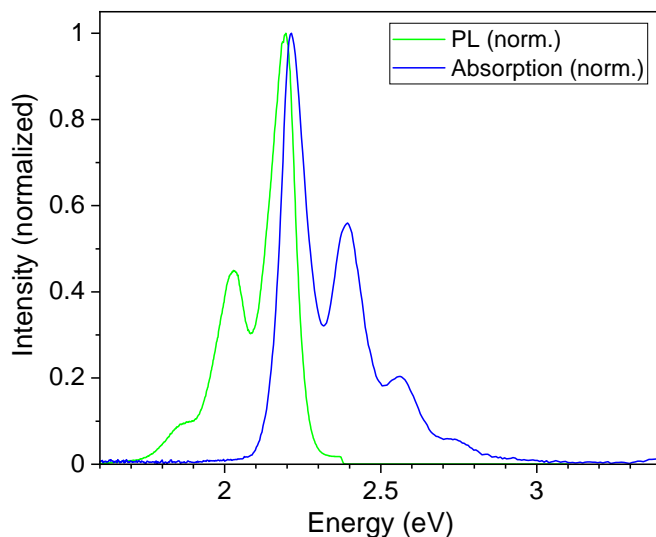


Figure 11: Static absorption (blue, right) and emission (green, left) spectra of terrylene in *para-xylene* solution. For the PL measurement, the molecule was pumped at 2.51 eV.

The absorption spectrum shows a major peak at 2.21 eV, which might belong to the electronic transition from the ground state  $S_0$  to the first electronically excited state  $S_1$ , or in case of an organic molecule from the HOMO to the LUMO. According to the Franck-Condon principle, transitions to higher lying vibronic levels appear as additional peaks at 2.39 and 2.56 eV on the higher energy side of the absorption spectrum. The well-resolved line-shape of the different vibronic transitions indicates strong vibronic coupling, which is typical for  $\pi$ -conjugated chromophores such as terrylene.

In accordance with the basic principles of spectroscopy, especially Kasha's rule, photoluminescence takes place from the lowest vibrational level of an electronically excited state to the vibronic progressions of the ground state. This leads to an emission spectrum, which is red-shifted and almost mirrored on the zero-phonon line compared to the absorption spectrum. As seen in Figure 11, this applies for the terrylene spectrum as well.

A major emitting transition appears at 2.03 eV, followed by peaks of the vibrational progression at 2.20 and 1.87 eV in the photoluminescence spectrum. The energy difference of 14 meV between the band maxima of the absorption and emission lines is defined as the Stokes-Shift. It mostly arises due to vibrational relaxation and solvent reorganization. During the fast transition to the excited state, the dipole moment of terrylene changes, but the solvent molecules are not able to adjust to that quick change, leading to a changed electronic environment and therefore a rise of the Stokes-shift. The small Stokes-shift observed here, can be explained by the vanishing dipole moment of *para*-xylene of 0 D.

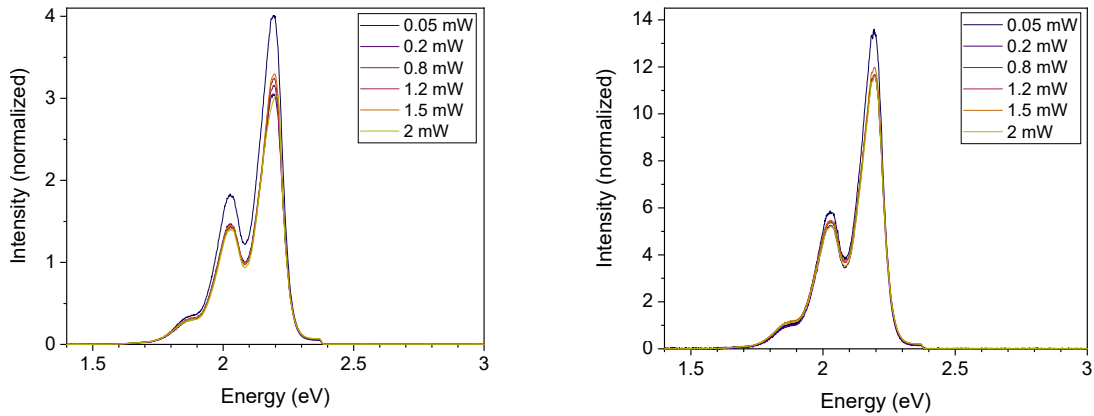


Figure 12: Static PL spectrum for Sample 1 ( $4\ \mu\text{M}$ , left) and Sample 2 ( $1\ \mu\text{M}$ , right), normalized with respect to the pump beam power.

To check for a possible non-linear behavior of the emission process, the photoluminescence spectra were measured with six different powers of the pump beam between  $50\ \mu\text{W}$  and  $2\ \text{mW}$  using a continuously variable neutral density filter. Normalizing the resulting spectra by dividing them by the applied power, as shown in Graph 12, allows to make statements about the fluence-dependence of the observed emission. The normalized graphs show almost the same shape and intensity for all powers and both samples. In other words, no fluence-dependence is observed and a linear process for the emission can be assumed. It is noticeable that for an excitation power of  $50\ \mu\text{W}$  the normalized spectra differ from the rest of the graphs. This can be explained by the really low power, where a small deviation in the power determination changes the resulting spectrum significantly. For Sample 1 the  $50\ \mu\text{W}$  graph differs by approximately 29%, for Sample 2 by roughly 17%. This lives up to an error regarding the power of the pump beam of  $14\ \mu\text{W}$  for Sample 1 or  $8\ \mu\text{W}$  for Sample 2. Compared to the other applied powers, this is negligible small and can arise due to unprecise adjustments of the filter or inaccuracies in the power measurement.

### 4.1.2 Time-correlated Single Photon Counting

In the last chapter, the electronic properties of terrylene were obtained from static measurements, which do not allow to get information about the temporal evolution of the different spectral features. To fully understand the electronic processes behind the terrylene molecule, discovering the dynamics of the excited state is important. To achieve this, time-correlated single photon counting (TCSPC) is used in the following chapter, to reveal the dynamics and lifetime of the observed emission.

The basic principle behind TCSPC measurements is explained in section 3.3. The terrylene sample is pumped with a photon energy of 2.51 eV, which is leading to the excitation of the sample and subsequently the emission of photons. Repeatedly measuring the time between the excitation and the detection of one single photon leads to a histogram of the electronic decay, which is shown in Figure 13.

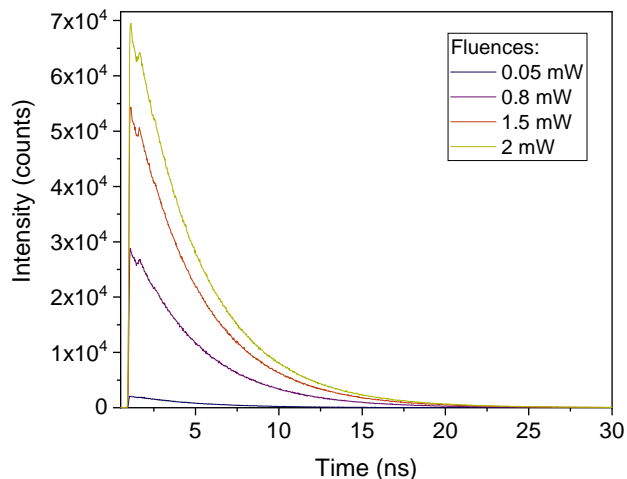


Figure 13: TCSPC traces of Sample 1 for different pump beam powers, excited at 2.51 eV.

To take into account the delay between the triggering of the photodiode and the real arrival time of the pulse at the sample, as well as the broadening of the spectral features, the underlying exponential decay function is convoluted with a so-called instrument response function (IRF) to yield the measured TCSPC trace. The instrument response function for the experimental setup used in this measurement was examined by B. T. Bonkano in previous works and is shown in Figure 14 a). According to that, the TCSPC trace is described by the following equation, which is used to fit the measured data later on:

$$I(t) = IRF(t) \otimes A \cdot e^{-\frac{t}{\tau}} \quad (4)$$

where  $I(t)$  is the measured intensity of the TCSPC trace and  $IRF(t)$  is the measured instrument response function. The decay of the excited state is described by the exponential decay function, where  $A$  is a parameter to adjust the intensity and  $\tau$  is the lifetime of the excited state.

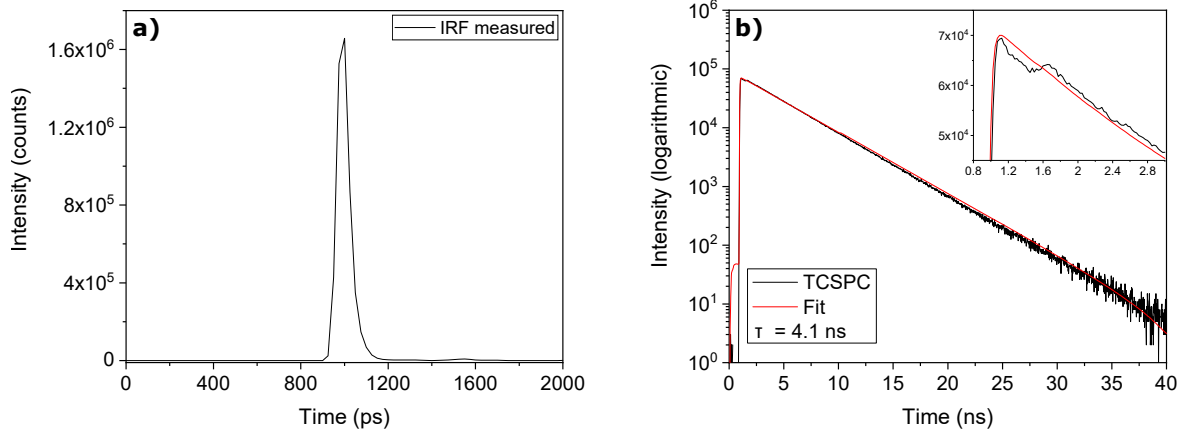


Figure 14: a) Measured instrument response function for the used setup, and b) TCSPC trace of terrylene with fit function and enlarged graph for early times in the inset.

To obtain the lifetime of the excited state, the decay traces were fitted according to equation (4) and plotted against a logarithmic y-axis, as shown in Graph 14 b). The resulting traces are perfectly linear, hence the decay is indeed described by a mono-exponential function and thus the fit model is validated. A lifetime  $\tau$  of 4.1 ns is obtained from the fit.

The fit is in very good agreement with the data. Nevertheless, as shown in the inset of Figure 14 b), the traces show an edge at 1650 ps which is not described by the measured instrument response function and therefore is not properly fitted. This could also explain why the fit function slightly overshoots the TCSPC trace at longer times.

Typically, such features either result from a reflection of the pump beam or from reflections of the emitted light, before it reaches the detector. Because this edge appears in all traces and for all samples at the same position, the reflection is probably resulting from the experimental setup and not from the cuvettes or samples itself.

To optimize the fit and take the echo into account, a second IRF is constructed. A reflection can be approximated by a second pulse in the IRF. This pulse is a scaled and delayed duplicate of the main pump pulse, which is visualized in Graph 15 a). Accordingly, the optimized fit function looks as followed:

$$I(t) = IRF_{constructed}(t) \otimes Ae^{-\frac{t}{\tau}} = (IRF_m(t) + B \cdot IRF_m(t + \Delta t)) \otimes Ae^{-\frac{t}{\tau}} \quad (5)$$

where  $IRF_m(t)$  is the measured instrument response function used above, and the additional parameters  $\Delta t$  and  $B$  correspond to the time delay between the main pulse and the reflected echo, and the intensity decrease of the duplicate, respectively. Gradually optimizing the constructed IRF and the fit of the exponential function, leads to a far better description of the observed reflection, as seen in the inset of Figure 15 b). According to the fit parameters, the second peak is shifted by 625 ps and is only 6% as strong as the major pump pulse. The time delay corresponds to a distance of  $\Delta s = c \cdot \Delta t = 19$  cm, which is a plausible distance for the experimental setup.

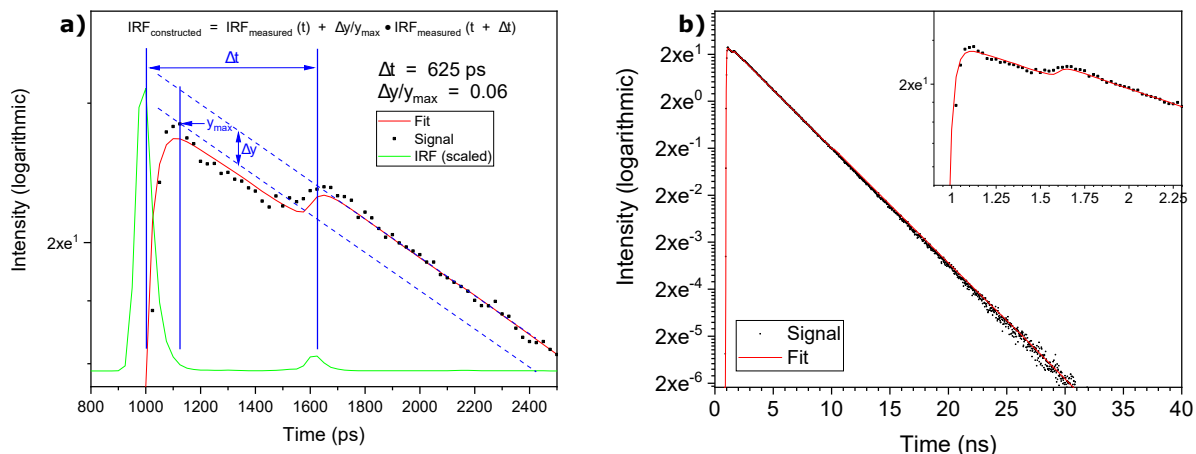


Figure 15: a) Explanation of the constructed IRF (IRF scaled for better visualization) and b) TCSPC trace with optimized fit according to equation (5).

Figure 15 b) shows the optimized fit with the constructed IRF. Besides the almost perfect description of the echo, the overall fit is improved for long times as well. This yields a lifetime of  $4.00 \pm 0.02$  ns for a mono-exponential decay of the excited state. Accordingly, the emission can be considered as fluorescence, which usually takes part during a few nanoseconds.

#### 4.1.3 Transient Absorption Spectroscopy and Electronic Dynamics

Using time-correlated single photon counting, we were able to determine a lifetime of  $4.00 \pm 0.02$  ns for the excited state. Because TCSPC only allows to observe emitting processes, the following chapter is about the evaluation of transient absorption spectra with an appropriate fit model. With this fit, it is possible to explain the complete transient absorption spectrum, just based on the static properties found out earlier. At first, the TA spectrum is briefly discussed, before the different components of the fit model are derived and the fit is applied to the measurement data.

The basic principles of transient absorption spectroscopy were introduced in chapter 3.4. TA spectroscopy is a pump-probe measurement technique, which allows to determine the differential absorption spectrum between an excited and unexcited sample. Moreover it allows to measure time-dependent data, by varying the time delay between the pump and probe pulse. In Figure 16, transient absorption spectra are shown for different time delays, both shortly after the excitation (top) and over a longer time period (bottom). For a better understanding of the following steps, the static absorption and photoluminescence spectra are additionally shown in the middle part of Figure 16.

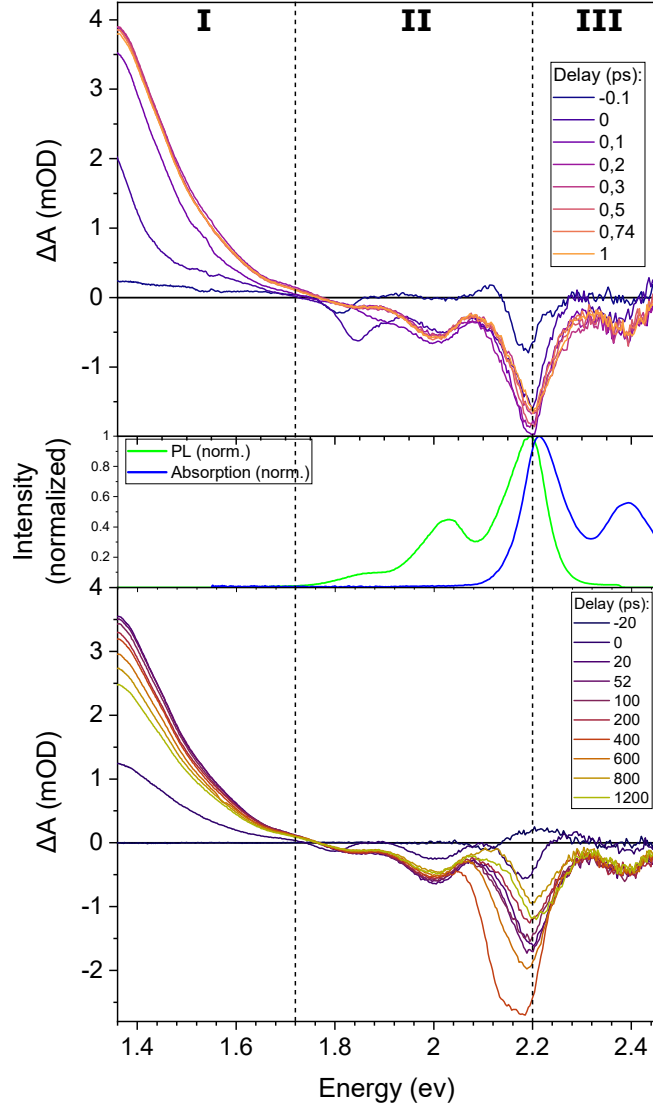


Figure 16: Transient absorption spectra at different pump-probe delays for terrylene in para-xylene solution. Top: Early times, Middle: Static absorption and photoluminescence spectra, Bottom: Long times.

The TA spectrum can be divided into three distinct areas, as shown in Graph 16. Area I contains a positive signal between 1.35 and 1.7 eV, which is coming from excited state absorption. Hence the static measurements do not show any signal in this spectral range, because excited state absorption can only occur in an excited sample. The shape of the curve indicates the presence of two separate features at around 1.35 eV and 1.5 eV.

Area II shows a negative signal in the range of 1.75 to 2.2 eV, with almost the same line shape and spectral position as the photoluminescence spectrum obtained from the static measurements. Therefore it can be assumed, that this spectral component corresponds to stimulated emission from the first excited state. It overlaps at 2.2 eV with a feature from the third area, which is a negative signal between 2.2 and 2.45 eV. The curve of this feature matches the lineshape and spectral position of the static absorption spectrum and hence is assigned as ground state bleach.

Furthermore, measuring the spectrum at different pump-probe delays allows to make statements about the temporal evolution of the different spectral features. The excited state absorption rises during 200 fs and then slowly decays on the order of several nanoseconds. Ground state bleach and stimulated emission show almost the same behavior. Noticeable is a very strong signal for the overlapping peak at 2.2 eV, which rises and decreases very fast around a pump-probe delay of 400 ps until it decays with the same dynamics as the other spectral components. Graph A.1 in the appendix shows the intensity of the TA spectrum at 2.2 eV against the pump-probe delay. According to that, the observed increase of the intensity is only a sharp peak and thus assumed to be a disturbance in the measurement setup, for example a vibration of the optical table, which changes the alignment of the beams and hence the pump beam could reach the detector. Because it only increases the signal at this specific delay, it is not considered in the following discussion anymore.

As already announced, a fit model for the TA spectrum was developed, which is capable of describing the different spectral features discussed above. This allows to explain the optical properties of terrylene molecules, as well as obtaining their dynamics. As shown in Figure 16, the TA spectrum contains three different signals. To properly describe the data, all of these features need to be considered in the fit function. To achieve this, the stimulated emission (SE) in area II is derived from the static photoluminescence spectrum, while the ground state bleach (GSB) signal in the third region can be obtained from the static absorption measurements. Therefore, the static spectra are fitted separately first. The resulting functions are then used to reflect the corresponding feature in the complete fit. The spectrum for the excited state absorption in area I cannot be derived from static measurements, because it is only present in an excited sample. Because the ESA signal is clearly separated and does not overlap with any of the other spectral features, it is represented by two Gaussian peaks.

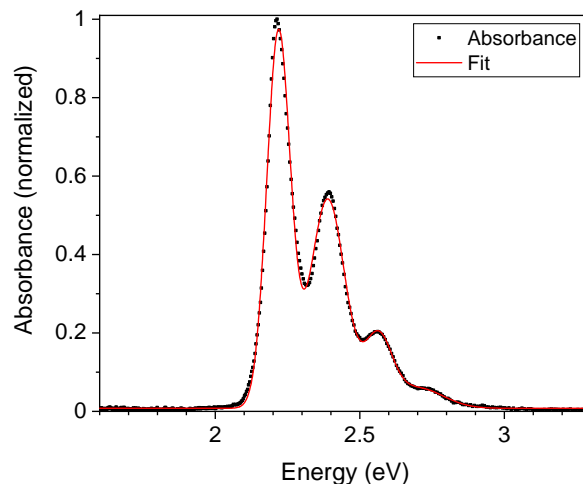


Figure 17: Static absorption spectrum (black) and fit (red) using four Gaussians.

In transient absorption spectroscopy, the negative signal of ground state bleach corresponds to the missing absorption of molecules in the ground state after the sample is excited by the pump beam. Therefore, the spectral shape of this component can be obtained directly from the static absorption spectrum. To achieve that, the spectrum is normalized to one to take into account the difference in intensities between the different measurement techniques and subsequently fitted using four Gaussians. The resulting fit in Graph 17 describes the line shape of the absorption spectrum properly with only minor deviations.

To receive the spectrum of the stimulated emission from the measured photoluminescence spectrum, the theory of Einstein coefficients is used.<sup>[4]</sup> According to this theory, the probability for a transition  $p_i$  depends on the Einstein coefficient  $A$  or  $B$  for the corresponding process and the number of molecules in the excited state  $N_j$ . Because the probability for a transition defines their intensity in a spectrum, the relation between photoluminescence and stimulated emission can be expressed as followed:

$$\frac{p_{SE}}{p_{PL}} = \frac{B_{21}N_2}{A_{21}N_2} \quad (6)$$

Because both transitions take place from the same excited state,  $N_2$  can be removed from the equation. Finally, the relation between the Einstein coefficients  $A$  and  $B$  is given by:

$$B = \frac{h^2 c^3}{8\pi e^2} \frac{1}{E^2} A \quad (7)$$

where  $h$  is the Planck constant,  $c$  the speed of light,  $e$  the elementary charge and  $E$  the photon energy in eV.

Using equation (6) and (7), the photoluminescence spectrum can now be converted into a stimulated emission spectrum and as in the case of the absorption spectrum, the curve is normalized and fitted using three Gaussians, as shown in Graph 18. As with the absorption spectrum, the fit properly reproduces the main features of the spectrum.

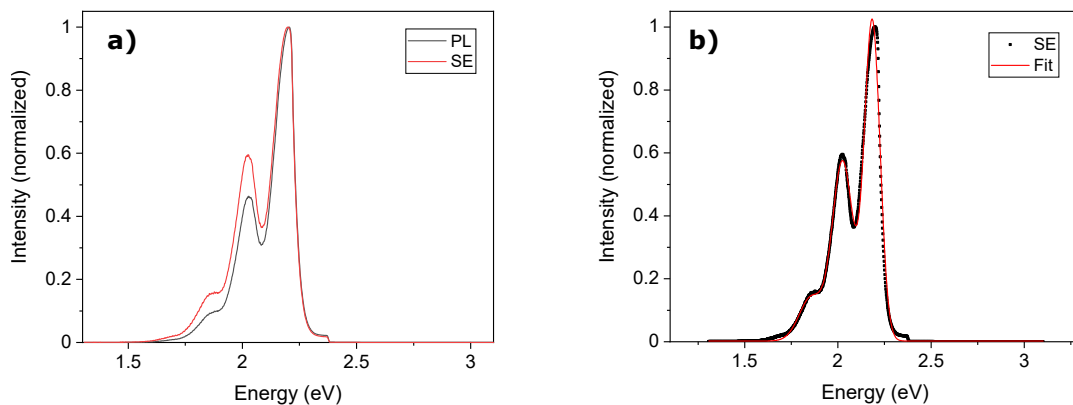


Figure 18: a) Comparison of photoluminescence and stimulated emission, based on the Einstein coefficients. b) Fit of the stimulated emission spectrum using three Gaussians.

Based on this results, the following equation (8) will be used to fit the TA spectra. As mentioned before, the two excited state absorption features are represented by two Gaussian peaks  $G$ , which are going to be optimized during the fit. The functions obtained from the fits above,  $I_{SE}(h\nu)$  for the stimulated emission and  $I_{GSB}(h\nu)$  for the ground state bleach, are directly used in the expression. They can only be changed in their intensity, by using the parameters  $SE$  and  $GSB$ .

$$I(h\nu) = G_1(h\nu) + G_2(h\nu) + SE \cdot I_{SE}(h\nu) + GSB \cdot I_{GSB}(h\nu) \quad (8)$$

Figure 19 contains an exemplary result of this fitting model. It should be noted that this rather coarse approach to describe the spectral properties of the TA spectrum is fitting the data surprisingly well. It is clearly shown that the signal in the spectral region between 1.75 and 2.45 eV consists of stimulated emission and ground state bleach, which are both obtained from static measurements. It is remarkable, that especially the fairly complex and overlapping data around the peak at 2.2 eV can be reproduced by the use of only two parameters.

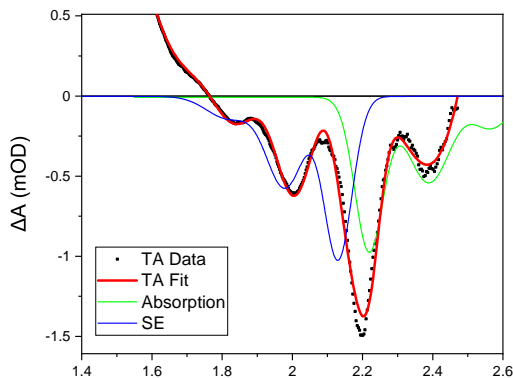


Figure 19: Visualization of the fit model (8), applied on the TA spectrum at a pump-probe delay of 100 ps.

While the excited state absorption is perfectly described by the two Gaussians, the fit shows some smaller deviations around the overlapping peak. To take into account energy shifts and spectral broadening due to the excited state of the molecule, additional parameters are introduced into the fitting equation. The functions to describe the stimulated emission and ground state absorption spectra consist of multiple Gaussians, where  $a_i$ ,  $b_i$  and  $x_i$  are obtained from the static measurements and keep unchanged during the following fit. Two additional parameter  $s_{SE}$  and  $s_{GSB}$  are used to allow a shift of the complete stimulated emission or ground state bleach spectrum, respectively. The parameters  $g_{SE}$  and  $g_{GSB}$  are able to reflect an uniform broadening of the spectra. According to that, the expanded fit equation has the following form:

$$I(h\nu) = a_{ESA,1} e^{-\frac{(x(h\nu) - x_{ESA,1})^2}{b_{ESA,1}}} + a_{ESA,21} e^{-\frac{(x(h\nu) - x_{ESA,2})^2}{b_{ESA,21}}} + SE \sum_{i=1}^3 a_{SE,i} e^{-\frac{(x(h\nu) - x_{SE,i} - s_{SE})^2}{b_{SE,i} g_{SE}}} + GSB \sum_{i=1}^4 a_{GSB,i} e^{-\frac{(x(h\nu) - x_{GSB,i} - s_{GSB})^2}{b_{GSB,i} g_{GSB}}} \quad (9)$$

The fit function (9) was applied to all measured pump-probe delays of the TA spectrum. In a first step, all parameters of the ESA Gaussians,  $SE$ ,  $GSB$  and the new degrees of freedom

$s_{SE}$ ,  $s_{GSB}$ ,  $g_{SE}$  and  $g_{GSB}$  are kept free. As before, for the stimulated emission and ground state bleach the parameters  $a_i$ ,  $b_i$  and  $x_i$  are taken from the fits of the static spectra and are not changed during the fitting procedure. Some of the resulting fits are exemplary shown in Graph 20.

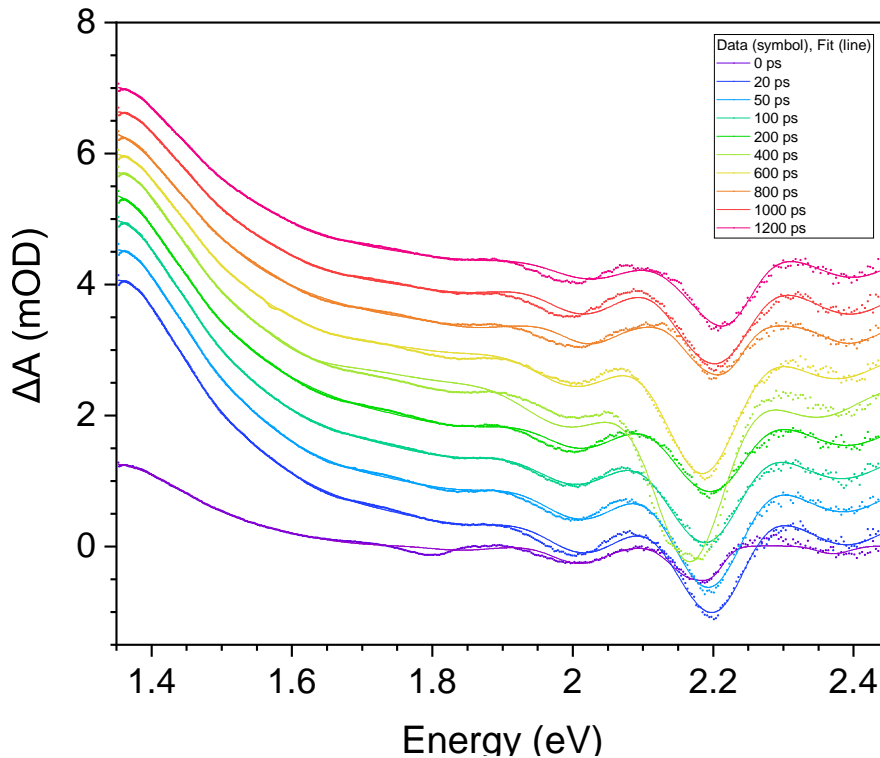


Figure 20: Batchfit results for selected pump-probe delays with fit equation (9).

The expanded fit model further improves the result. The excited state absorption is still well described and due to the additional parameters, the overlapping region of stimulated emission and ground state absorption matches the data even better than before. Almost perfectly fitting the whole transient absorption spectrum of terrylene in *para*-xylene solution with only six parameters for the stimulated emission and ground state bleach is noticeable, as it shows that the electronic properties of single terrylene molecules can be easily understood using the static measurements.

Besides reflecting the data, the batchfit results can now be used to extract further information about the different parameters and their temporal evolution. The important parameters resulting from the batchfit are shown in Figure 21. Due to the strong correlation of the two partially overlapping Gaussians which make up the excited state absorption, the corresponding parameters are very unevenly distributed and therefore not shown or discussed.

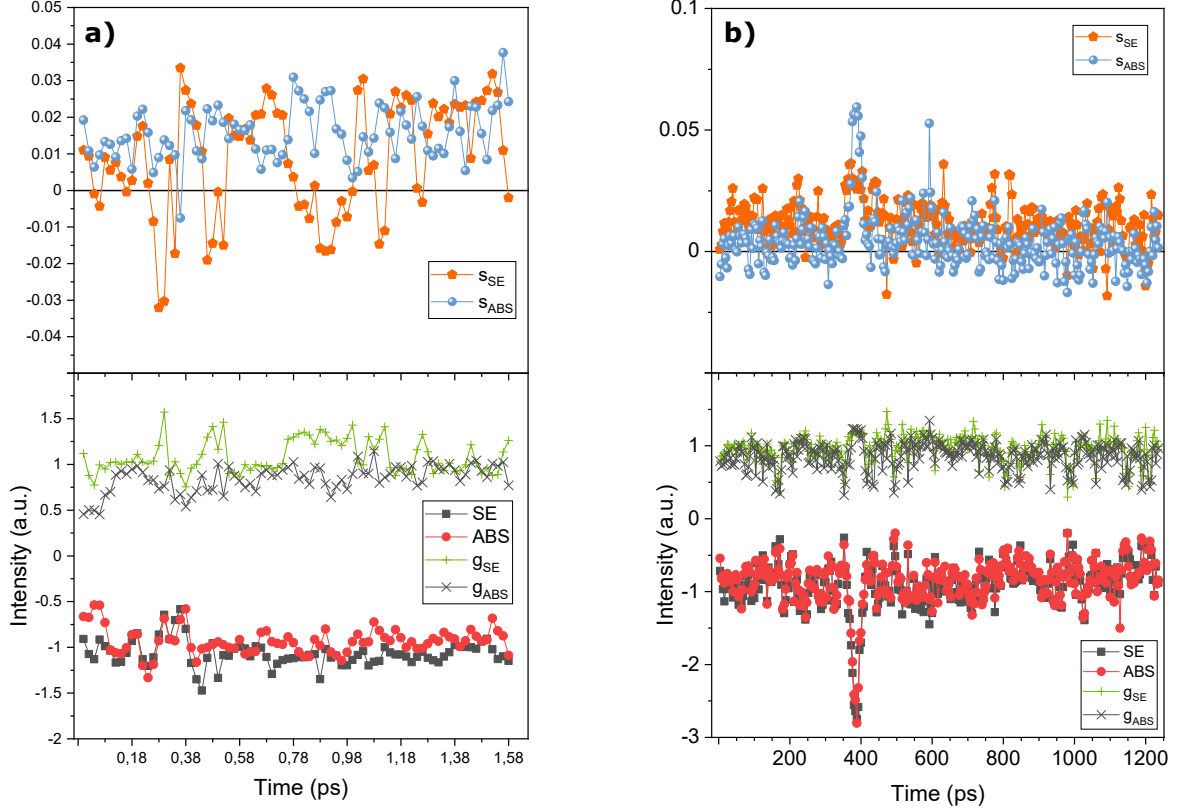


Figure 21: Parameters from batchfit for early (a) and long (b) times.

The parameters  $g_{SE}$  and  $g_{GSB}$  for scaling the bandwidth of the stimulated emission and ground state bleach spectra are mostly around or lower than one, indicating that the peaks in the TA spectrum are narrower than the peaks from the static measurements. In the static measurements a small spot of the sample is excited over a long time, while in the TA measurement the excitation is discontinuously, allowing for a more homogeneous distribution of the excited molecules, which could result in a smaller bandwidth.

The shift of the stimulated emission spectrum  $s_{SE}$  lays between 0 and 25 meV and thus is a blueshift. At early times, the absorption spectrum is blue-shifted between 0 and 20 meV. After approximately 600 ps, the shift is getting smaller and the ground state bleach becomes slightly red-shifted. This could be explained by the temperature increase which is caused by the excitation beam, resulting in the population of higher vibronic levels. Accordingly, the absorption happens from higher vibronic levels of the ground state, leading to a lower energy of the transition, while the emission happens from higher vibronic levels of the excited state and therefore has higher energies. This could also explain the changes in the GSB shift over time, because the temperature decreases after the excitation and leads to the fast relaxation of higher vibronic levels, reducing the blueshift of the absorption.

Especially interesting is the temporal evolution of the parameters  $SE$  and  $GSB$  as shown in Graph 21, which correspond to the dynamics of the associated spectral processes. Both transitions show almost the same intensity and a slow decay over several nanoseconds. Taking into account the simplified fit model used for describing the physical origins of those signals, it is notable how the pure parameters  $SE$  and  $GSB$  reflect the temporal evolution of stimulated emission and ground state bleach with just a moderate spreading of the data points. Compared to the lifetime of the excited state, which is approximately 4 ns according to the TCSPC data, the TA was only measured up to a pump-probe delay of 1.2 ns and consequently is not showing the full decay. Additionally, the temporal resolution is not sufficient enough to resolve the rise of both signals, which is happening during a few hundred femtoseconds. Nevertheless, with the high quality of the obtained parameters, we are able to prove the validity of our fitting procedure.

Another advantage of the previous fit is, that the composition of the TA spectrum is uncovered, allowing to assign almost pure signals for stimulated emission at 2 eV and for the ground state bleach at 2.4 eV. By plotting the intensity of the TA signal at this specific energies against the pump-probe delay, the temporal evolution of the spectral processes can directly be obtained from the data. Figure 22 shows those kinetic traces for the stimulated emission and the ground state bleach, as well as for the excited state absorption, which are taken at 1.35 eV and 1.67 eV.

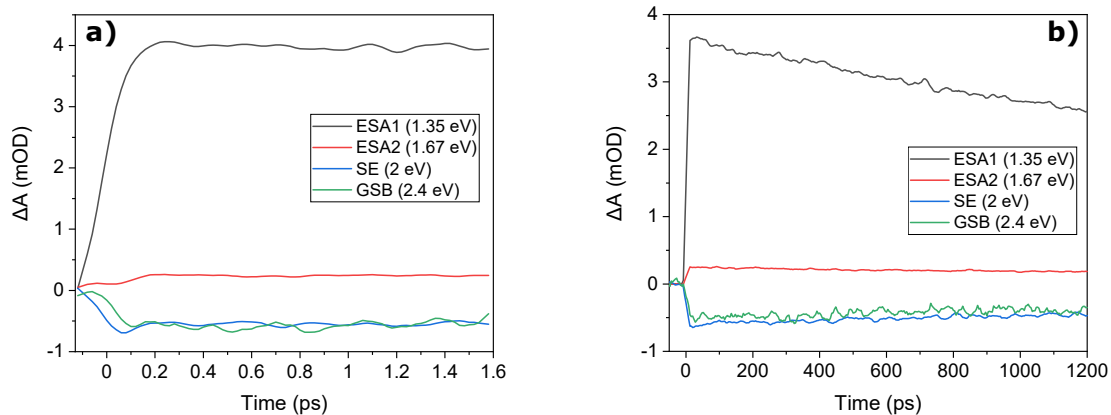
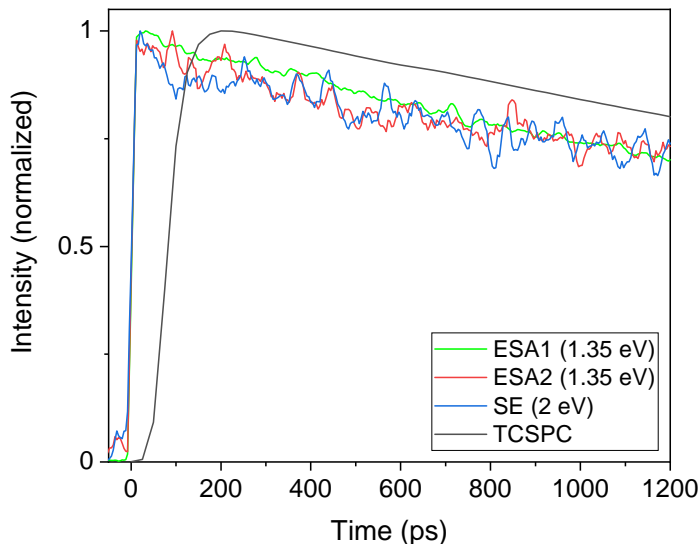


Figure 22: Early (a) and long (b) dynamics of the different spectral features in the TA spectrum.

The traces allow more precise statements about the electronic dynamics and confirm the temporal evolution observed in the spectra and in the fit parameters. The different spectral components rise during approximately 200 fs and decay on the order of several nanoseconds. Exemplary fitting the ESA1 trace, which has the best signal-to-noise ratio, with a mono-exponential decay reveals a lifetime of  $4.6 \pm 0.86$  ns for the excited state. The short measuring time of only 1.2 ns compared to the assumed lifetime, leads to a relatively high uncertainty, but the result is still in coincidence with the lifetime obtained from the TCSPC measurement.

Graph 23 shows the normalized kinetic traces from Graph 22, as well as the TCSPC trace. It is clear to see that all spectral components follow the same dynamics and therefore can be assigned to the same excited state. Furthermore it shows, that the dynamics which were obtained from the TA and from the TCSPC measurements are in accordance with each other. This not only validates the data from both measurements, moreover it allows to assign the precise lifetime of  $4.00 \pm 0.02$  ns obtained from the TCSPC to the TA data and hence to all spectral features.



*Figure 23: Kinetic traces from TA spectra, all normalized to one. For better comparison, the TCSPC trace was calculated from the obtained exponential decay function convoluted with the measured IRF, to remove the observed edge.*

## 4.2 Discussion of Single Molecule Behavior

In the previous chapters, the behavior of single molecules of terrylene in solution was discussed. For future developments it is important to fully understand the electronic properties of a material. Therefore, a simple and well-known molecule is desired.

From the perspective of the conducted measurements, terrylene behaves like a textbook molecule. Static and transient absorption spectroscopy show three major transitions, including ground state absorption at 2.21 eV and a strong, Stokes-shifted fluorescence at 2.03 eV. Both processes have a well resolved line shape, corresponding to the transitions from and to different vibrational levels of the electronic states. In the TA spectrum, the absorption and emission are present as ground state bleach and stimulated emission. The transient absorption spectra additionally contain a broad excited state absorption band, with pronounced features at around 1.35 eV and 1.5 eV. As discussed earlier, there are no signs for non-linear processes in the terrylene molecule.

An exact lifetime of the excited state can be received by fitting the TCSPC trace with an appropriate fitting function, yielding a lifetime of  $4.00 \pm 0.02$  ns for a mono-exponential decay. Subsequently, the transient absorption data was fitted with functions for the ground state bleach and stimulated emission, which were obtained from the static measurements. It is especially notable, that the fits are in very good agreement with the data, both in the energy and temporal domain. Furthermore, this allows to extract information about the temporal evolution of the different spectral processes. It was shown, that all transitions follow the same dynamics and hence are belonging to the same electronically excited state.

Starting from this, the following energy level diagram in Scheme 24 for single terrylene molecules can be assumed. Since this is a relatively simple system, containing strong and well-resolved transitions, terrylene can be titled a textbook-like molecule. As already mentioned, this is favored for the development of new materials and applications, because it allows to easily understand the properties of the molecule. Especially in HIOS devices, where multiple materials are interacting, the properties of a single component should be as simple as possible. Particularly the strong absorption in the UV-Vis region as well as the long lifetime of the excited state, makes terrylene a promising candidate for potential applications in light-harvesting or opto-electronics.

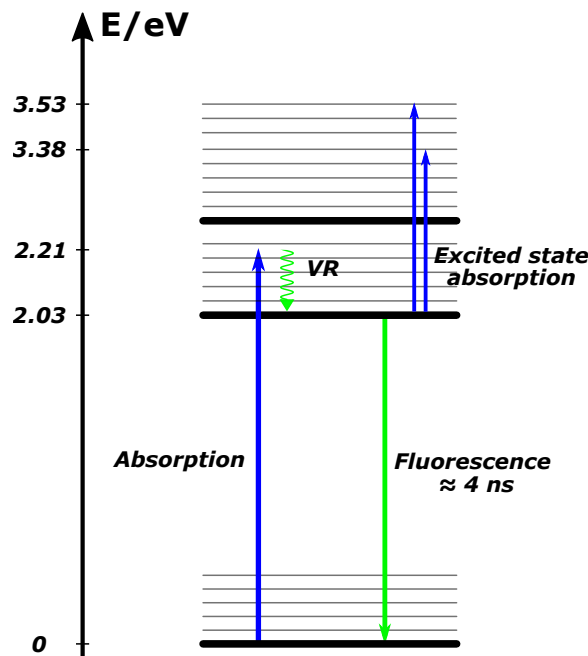


Figure 24: Energy level diagram for single terrylene molecules in solution (schematically). Major transitions shown as arrows.

### 4.3 Thin Films of Terrylene

After the single molecule behavior was thoroughly discussed in the previous sections, the following chapter will cover the steady state properties of thin films of terrylene on fused silica. Most applications, for example in the opto-electronic field, require their materials to be in a solid state. Changes in the electronic properties between a molecule in solution and in solid films are common and sometimes even desirable, if they result in new advantages and possibilities for the design of particular devices, but they rise the need for extensive investigations of the solid state properties. Compared to the relatively simple and textbook-like behavior of the single molecule, thin films of terrylene show a much more complex behavior, regarding their optical properties and electronic transitions, as well as their dynamics. Chapter 4.3.1 is about the static absorption of this films, especially showing a strong blueshift compared to the monomer absorption, which is assigned to the formation of H-aggregates. Subsequently, in section 4.3.2 and 4.3.3, a fitting model is introduced and applied, which is capable of explaining the different spectral components that make up the TA spectrum, as well as their temporal evolution. It is notable that the fit is in very good agreement with the data, only with the use of a small number of parameters and functions from the static measurements. Particularly interesting is the formation of induced monomers, since it shows the possibility to modify aggregates on an ultrafast timescale.

#### 4.3.1 H-Aggregate Formation in Thin Terrylene Films

The condensation of molecules can lead to a variety of changes in their properties. Especially organic chromophores, like terrylene, tend to form aggregates in close spacial proximity. According to Kasha's theory, which was introduced in chapter 2.3, depending on the alignment of the transition dipole moments, two types of aggregates can occur. While the formation of J-aggregates with a head-to-tail arrangement of the transition dipole moments results in an energetic lowering of the excited state and thus a redshift of the absorption wavelength, H-aggregates occur in molecular crystals with a parallel arrangement of the transition dipole moments. This mainly results in a blueshift of the absorption, as well as strong fluorescence quenching. Besides this two extreme cases, an oblique arrangement of the transition dipole moments can lead to mixed aggregates or it is possible that there is no aggregation and the solid shows a monomer-like behavior.

To investigate the ground state absorption and hence the possible formation of aggregates in thin terrylene films, static absorption spectroscopy is used. The resulting, normalized spectrum is shown in Graph 25, in comparison to the single molecule absorption spectrum.

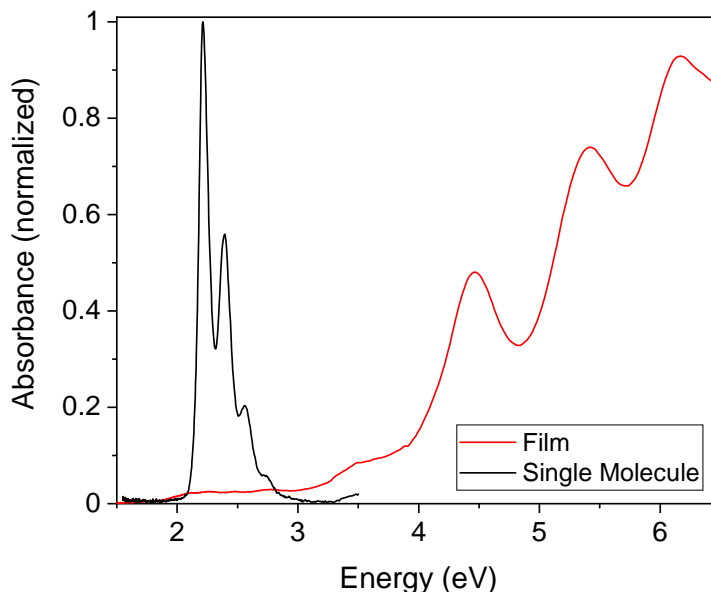


Figure 25: Normalized, static absorption spectra of single molecules in *para-xylene* (black) and thin films of *terrylene* (red).

Clearly, the thin film response is very different compared to the single molecule absorption. The absorption spectrum of the *terrylene* film shows a broad band with a band maximum at 6.15 eV. On the lower-energy site of the band, multiple peaks appear with a line spacing of  $0.89 \pm 0.15$  eV.

Compared to the single molecule spectrum there are three major differences. First, the whole absorption spectrum is strongly blue-shifted into the UV-region. Another significant difference is the changed line shape, particularly a change in the amplitude and a strong broadening of the individual bands. Additionally, the films do not show any photoluminescence, neither for excitation in the visible nor in the UV. This is in contrast to the single molecule, which has a strong fluorescent transition with a fairly long lifetime.

According to that observations, we assume the formation of H-aggregates in thin *terrylene* films, as it explains the strong blueshift. Prerequisite for the formation of H-aggregates is a parallel, stacked arrangement of the molecules. Therefore, it is assumed that the *terrylene* molecules form a herringbone structure. Because a solid film contains a large number of interacting molecules within these kinds of fixed arrangements, a variety of vibronic states arises, leading to a broadening of the absorption bands. Nevertheless, this cannot explain the peak progression, because a line spacing of approximately 900 meV is most likely not coming from vibrational modes.

Finally, the missing photoluminescence can also be explained by the H-aggregate formation. Kasha predicted, that rapid inter-vibrational relaxation takes place before the emission, so that photoluminescence always occurs from the lowest excited state. But in the case of H-aggregates, the transition to or from the lower energy state is dipole-forbidden, resulting in a strongly reduced fluorescence and a non-radiative decay.

### 4.3.2 Induced Monomer Absorption

In the last section, the steady state electronic properties of thin terrylene films were examined, revealing the formation of H-aggregates and the associated blueshift of the absorption wavelength. Transient absorption spectroscopy allows to investigate additional spectral processes, which are not directly associated with the ground state. Transient absorption spectroscopy was already performed for the single molecules, showing the presence of a well understood, textbook-like molecule. In fact, thin terrylene films are much more complex and perform a variety of other electronic processes. As mentioned earlier, solid state materials are usually required for real-life applications, resulting in the need to understand how the condensation of such molecules changes their optical and electronic properties. Besides the already discovered H-aggregate formation, it is especially interesting if those aggregates can be manipulated.

In the following chapter, the transient absorption spectrum of solid state terrylene is analyzed, to investigate the underlying spectral processes and gain a more extensive understanding of the TA spectrum, which is required for the subsequent fitting procedure in chapter 4.3.3. Especially remarkable are two features in the film, on the one hand a shifted ground state absorption which is overlapping with the traditional ground state bleach, and on the other hand the ultrafast generation of induced monomers, which show a monomer-like absorption spectrum.

Graph 26 b) contains the transient absorption spectra of thin terrylene films on fused silica for different pump-probe delays. Additionally, the ground state absorption spectra of the monomers and the film are shown in the upper panel a), to facilitate the following discussion.

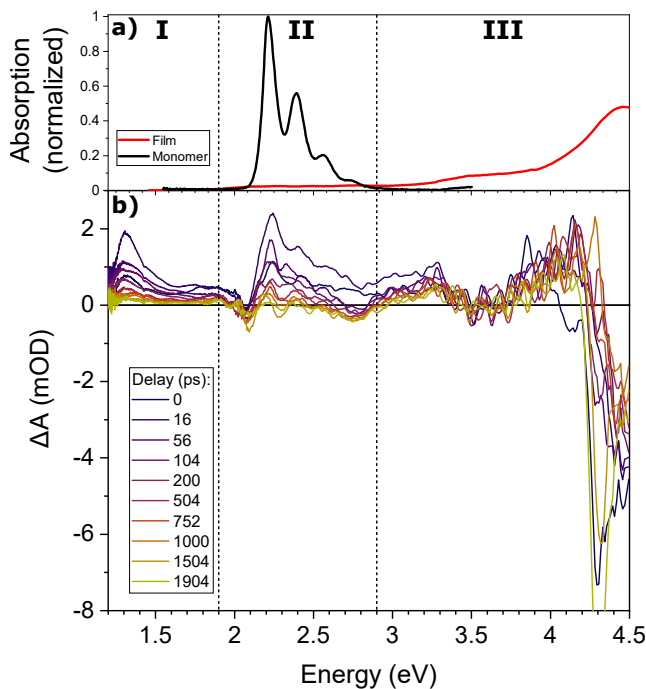


Figure 26: a) Ground state absorption spectrum for terrylene monomers and films. b) Transient absorption spectra of terrylene films (50 nm) at different pump-probe delays. Area I: Excited state absorption, Area II: Induced absorption, Area III: Ground state absorption signal.

As already mentioned, the TA spectrum is much more complex and contains more features than the monomer response. To structure the discussion, it is feasible to divide the spectrum into three areas, as indicated in Graph 26.

On the lower energy side of the spectra, in area I, a positive band occurs with a maximum at 1.3 eV. Since the signal is positive and neither the monomer nor the film absorption spectrum shows any response in this spectral range, this feature is assigned to excited state absorption. The small kink at 1.43 eV corresponds to third order grating of the pump beam with an original energy of 4.28 eV. Thus, the excited state absorption does not show any signs of multiple, overlapping signals.

Another, more complicated signal can be seen in area III between 2.8 and 4.5 eV. It consists of negative signals around 3.5 eV and from 4.3 to 4.5 eV, in between the signal is positive. If one pays attention to the spectral position of these features, this region should contain the ground state bleach, as expected from the static absorption measurement shown in the upper panel. Consequently, the ground state bleach needs to overlap with another signal to yield the observed line shape. The composition of this feature is further investigated using a fitting procedure in chapter 4.3.3, showing that it is indeed coming from the ground state absorption. It will be shown that the GSB signal overlaps with a red-shifted duplicate of the ground state absorption spectrum.

Especially interesting is the positive signal in area II between 2.1 and 2.8 eV, which matches the spectral position and roughly the line shape of the monomer absorption shown in panel a). This is surprising, because the static absorption spectrum of the film does not show any monomer-like response, instead the already discussed H-aggregate formation. According to that, the monomer response in the TA spectrum cannot come from residual monomer units. Paying attention to the basic principles of TA spectroscopy, a positive TA signal requires absorption in an excited state, and no or weaker absorption in the molecules ground state. Since the monomer signal is positive, the absorption needs to take place after the photoexcitation. The excitation with a photon energy of 4.28 eV is above resonance and is bringing a lot of heat into the sample. We assume that this excess energy is dispersed onto adjacent molecules and aggregates, which could then lead to a destruction of the aggregates, resulting in the formation of induced monomers. Consequently, their absorption is called *induced monomer absorption*.

On the low-energy side of the induced absorption band, a relatively small, negative signal is visible. With regard to the spectral position, slightly red-shifted to the induced monomer absorption and the matching position of the monomer fluorescence, it is assumed that this signal could be stimulated emission from the induced monomers. Unfortunately, the signal is very weak and overlaps with the induced monomer absorption, the excited state absorption as well as the second order grating of the pump beam at 2.15 eV. That is why the signal cannot be assigned as stimulated emission for sure.

Investigating and explaining the spectral properties of thin terrylene films is complicated, as there are multiple transitions and processes, which are not as distinct compared to the properties of single molecules in solution. There are mainly two components which appear in the spectra. On the one hand, aggregated molecules which form H-aggregates, as indicated by the strong blueshift of the ground state absorption spectrum and the missing photoluminescence of the film sample. On the other hand, the TA spectra show the presence of induced monomers after the photoexcitation, which resemble the properties obtained for the single molecules, especially regarding their ground state absorption and possibly also a weak stimulated emission. This is notable, because it shows the possibility to modify and break aggregates on an ultrafast timescale, which, for example, increases the flexibility in the development of hybrid inorganic-organic devices, since it allows the terrylene film to absorb light almost over the complete spectral range from 2 to 6 eV.

### 4.3.3 Ultrafast Dynamics of Terrylene Films

The previous section showed the presence of multiple spectral components in the transient absorption spectrum, most prominent a monomer-like absorption feature and a composed ground state bleach signal. To further understand the origin and physical explanation of these signals, a fit model is applied to the TA data in the following chapter. It will be shown, that those spectral regions can be described in very good agreement with the data, just by using the static absorption spectra and a small number of parameters. Furthermore, the fit parameters resulting from the fit, as well as kinetic traces obtained directly from the TA spectra are used to examine the dynamics of the different processes.

To establish an appropriate fit function, all relevant physical processes need to be included. They were already discovered in the previous section and are now mathematically modeled. In Graph 26, the terrylene film spectrum is divided into three major parts. Area I only contains signals from the excited state absorption, hence it is not relevant for the discussion of the other important features and will be ignored in the following fit.

The remaining areas II and III are shown in Graph 28 again, including all components of the fit function. Area II contains the induced monomer absorption. According to our interpretation, this feature is resulting from ground state absorption of monomer units and as shown in panel a) of Graph 26, it has roughly the same spectral position and line shape as the static absorption spectrum of the monomers. Consequently, in the fit the induced monomer absorption  $IMA(h\nu)$  (blue) is represented by the fit function of the single molecule, which was derived in chapter 3.1.3. To take into account the small edge on the low-energy side of the induced monomer absorption band, which is assumed to be a stimulated emission signal, a negative Gaussian  $SE(h\nu)$  (purple) is added to the fitting function.

According to the ground state absorption spectrum shown in the upper panel of Graph 26, area III should contain the ground state bleach. Obviously, the line shape in this area strongly differs from the ground state response. It was discovered that the actual signal is an overlap between two signals, which is resulting in this kind of complicated line shape. To understand how this signal arises, it is necessary to remember the basic principle of transient absorption spectroscopy, which is further explained in section 3.4. A TA signal is defined as the difference between the absorbance of an excited sample and the absorbance of the sample in the ground state. The ground state absorption is only happening for unexcited molecules, hence the absorbance at this spectral position is positive for the molecule in the ground state and zero for an excited molecule. Consequently, the resulting TA signal of the ground state bleach  $GSB(h\nu)$  (green) will be negative.

We found out, that the overlap of the GSB signal with a second absorption signal, which is positive and slightly red-shifted, is able to reproduce the observed line shape. We assume, that this signal is coming from modified aggregates after the photoexcitation. Accordingly, the ground state absorbance is zero and after the photoexcitation a positive absorbance arises. Consequently the *modified aggregate absorption* signal  $MAA(h\nu)$  (orange) would be positive. Summarized, the TA signal  $I(h\nu)$  for area III is calculated as the difference between the unpumped (up) and pumped (p) sample, as followed:

$$\begin{aligned} I(h\nu) &= A_p(h\nu) - A_{up}(h\nu) = A_{GSB,p}(h\nu) + A_{MAA,p}(h\nu) - A_{GSB,up}(h\nu) - A_{MAA,up}(h\nu) \\ &= 0 + A_{MAA,p}(h\nu) - A_{GSB,up}(h\nu) - 0 = MAA(h\nu) - GSB(h\nu) \end{aligned} \quad (10)$$

In the pumped sample, only the modified aggregates (MAA) will absorb, while absorption in the unpumped sample is only coming from unmodified aggregates (GSB).

To yield a function  $GSB(h\nu)$  for the ground state bleach, the static absorption spectrum of the terrylene film is fitted using four Gaussian peaks. The obtained fit is shown in Graph 27. Despite smaller deviations it is in good agreement with the data. To obtain the function for the modified aggregate absorption  $MAA(h\nu)$ , the fitted ground state bleach spectrum is shifted by a variable energy shift  $\Delta E$ :  $MAA(h\nu) = GSB(h\nu + \Delta E)$ .

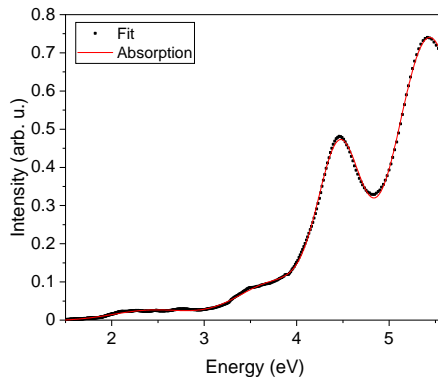


Figure 27: Fitting the static absorption spectrum for the terrylene film.

Combining all four components mentioned above, results in the following fit equation for the film TA spectrum:

$$I(h\nu) = A \cdot MAA(h\nu) - B \cdot GSB(h\nu) + C \cdot IMA(h\nu) + D \cdot SE(h\nu) \quad (11)$$

Equation (11) is now used to fit an exemplary TA spectrum, as shown in Graph 28. In the first step, the parameters  $A$ ,  $B$ ,  $C$  and  $D$ , the energy shift  $\Delta E$ , as well as the two parameters for the  $SE$  Gaussian are kept free. First of all it is remarkable, that this complicated spectrum can be represented by a fit, which is only using ground state spectra and a small number of parameters. Because the stimulated emission signal leads to only small changes on the lower-energy side of the induced monomer absorption band, the three parameters of the Gaussian are not relevant for the majority of the features seen in area II and III. Accordingly, those areas are described by only four parameters. In area III the fit shows some deviations from the data. Nevertheless it should be noted, that the fit still allows to explain the composition of the spectral feature in area III, by using just two components and three parameters. During the fit of multiple datasets, a best working redshift between the GSB and MAA signals of 220 meV was obtained. This value is fixed in the following fitting procedure, to allow a more evenly distributed result for the kinetic parameters  $A$  and  $B$ .

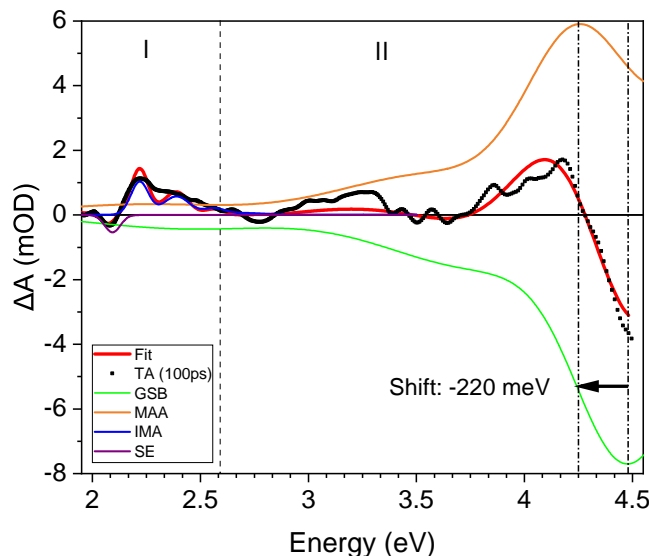


Figure 28: Exemplary fit for the TA spectrum at a pump-probe delay of 100 ps using equation (11). The different components of the fitting model are visualized.

In the previously shown fit, using equation (11), the spectral position of the induced monomer absorption is in good agreement with the monomer absorption spectrum, despite the fact, that the IMA bands are not as well resolved as the monomer spectrum. To account for that, an additional parameter  $g_{IMA}$  is introduced, to allow a uniform broadening of the bands. Accordingly, the following function is subsequently used for the induced monomer absorption in the fit model:

$$I_{IMA}(h\nu) = \sum_i a_i \cdot e^{-\frac{(E - x_i)^2}{(g_i \cdot gIA)^2}} \quad (12)$$

where the parameters  $a_i$ ,  $x_i$  and  $g_i$  are kept unchanged and correspond to the fit parameters of the monomer absorption spectrum. The use of additional parameters to optimize the result was tried out as well. Even if they are capable of enhancing the match between the fit and the data for some time delays, no systematic improvement was found. Therefore, they are not used in the fit model, to allow a physical meaningful interpretation of the obtained parameters.

This optimized fitting procedure is now used, to fit the TA spectra for all pump-probe delays. In Graph 29, the TA data and corresponding fits are shown for some exemplary delays. The fits of more time delays can be found in the Appendix A2. Due to the modification of the fitting procedure, the fit in area II matches the TA signal almost perfectly. While there are some deviations around the signals at 4.25 eV and between 2.8 and 3.5 eV, the fit is well describing the whole spectrum for all time delays. This fit uses only two functions from the static measurements and eight parameters, four for the amplitudes  $A$ ,  $B$ ,  $C$  and  $D$ , the spectral broadening parameter  $g_{IMA}$ , two parameters for the SE Gaussian and the fixed energy shift of  $\Delta E = 220$  meV. This is an outstanding result, as it shows, that the composition of this complicated signals in area II and III can be described for all pump-probe delays by only five parameters, if the stimulated emission is excluded. It was already explained, that simple molecules are preferred for demanding applications, as they allow to fully understand the system that is built. With this fit, we accomplished a far better understanding of the electronic properties of thin terrylene films, which can help in future scientific works.

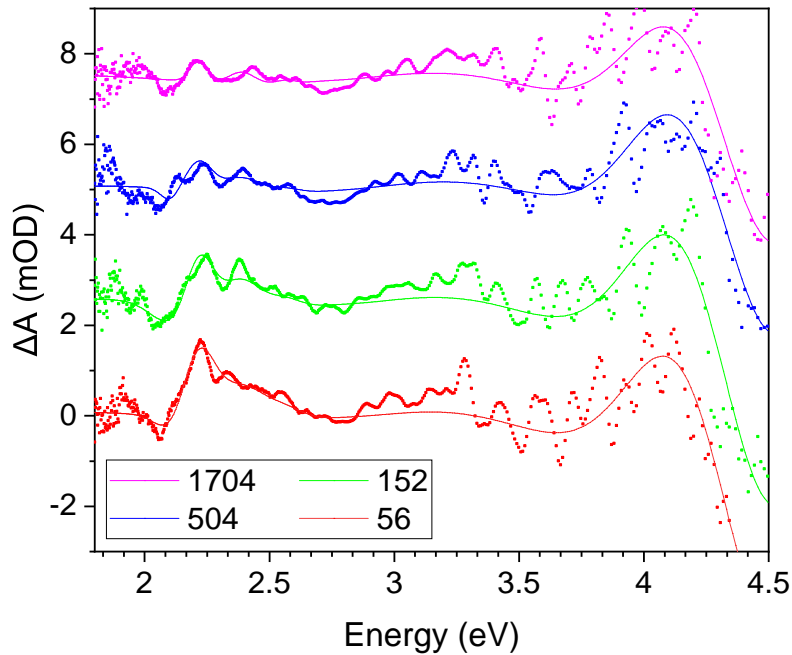


Figure 29: Exemplary fits for the thin terrylene film TA spectrum.

By fitting the spectra for all pump-probe delays, the temporal evolution of the parameters  $A$ ,  $B$ ,  $C$  and  $D$  were obtained. According to equation (11), the parameters correspond to the amplitudes of the different spectral components. Consequently, plotting the parameters against the pump-probe delay corresponds to kinetic traces of the individual spectral features. Graph 30 shows the temporal evolution of the parameter  $B$  for the ground state bleach (black), parameter  $A$  for the modified aggregate absorption (red) and parameter  $C$  for the induced monomer absorption (blue) for early pump-probe delays with a step size of 20 fs. Due to the low intensity of the stimulated emission, the parameter  $D$  is not considered in the following discussion.

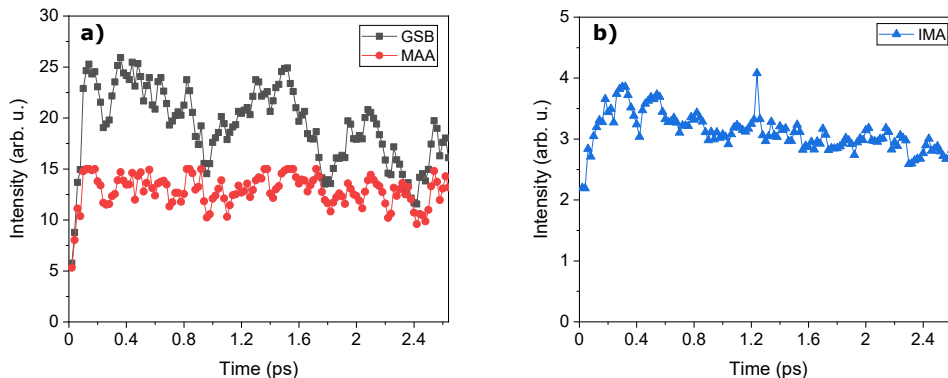


Figure 30: Early dynamics of the TA spectral components, GSB and MAA in panel a and IA in panel b.

Notable is the high quality of the obtained fit parameters, which show the rise and decay dynamics with a relatively good signal-to-noise ratio. The ground state bleach (black) and the modified aggregate absorption (red) both rise within approximately 150 fs, i.e. on the order of the time resolution. In comparison to these features, the induced monomer absorption clearly shows a delayed rise within roughly 400 fs. Unfortunately, the temporal resolution of the TA measurement is not sufficient enough, to determine an exact rise time or even fit the rise dynamics.

During the early times, all three components seemingly show a mono-exponential decay, with a lifetime of several picoseconds that exceeds the observed time frame significantly. The pure ground state bleach signal is very noisy, therefore a tangible comparison with the dynamics of the modified aggregate absorption is not feasible at this point.

By fitting the TA spectra with a larger step size of 8 ps, further information about the long-time evolution of the spectral features can be obtained. The kinetic traces for the GSB, MAA and IMA are shown in Figure 31. It is especially interesting, that those dynamics are much more complex than in the single molecule, where all spectral processes had the same temporal evolution. Compared to the early dynamics, the parameters are more evenly distributed and the larger time frame even allows to fit the decay traces with a sufficient uncertainty.

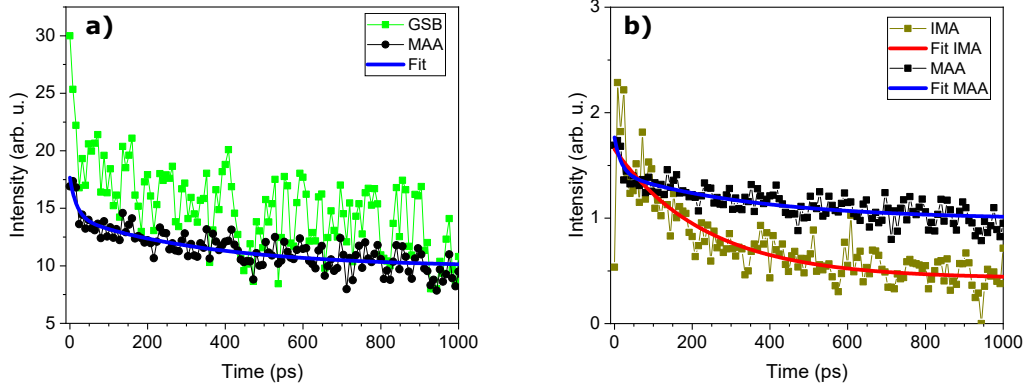


Figure 31: Kinetic traces obtained from batch fitting the TA data. Panel a: GSB (gray), MAA (red) and fit of the MAA decay (black). Panel b: IA (black) and MAA (gray) and corresponding fits of the decay.

While the dynamics of the induced monomer absorption are clearly different, the ground state bleach and modified aggregate absorption both seem to have the same temporal evolution. In Figure 31, the GSB and MAA features show an instantaneous rise on the order of the time resolution, followed by a bi-exponential decay with two distinct lifetimes. Consequently, the relaxation needs to involve two different species or decay pathways. If one pays attention to the higher intensity of the GSB, both the ground state bleach (green) and modified aggregate absorption (black) seem to have the same dynamics on the order of tens or hundreds of picoseconds for the fast and slower decay component, respectively. Compared to that, the decay of the induced monomer absorption (brown) seems to be a mono-exponential decay which is slightly faster than the longer component of the other features. All three processes show a final, extremely long living decay component on the order of several nanoseconds, which is clearly exceeding the measured time frame.

To extend this investigation with quantitative values, the decay traces are subsequently fitted. The resulting decay traces are shown in Figure 31 and are summarized in Table 1. The GSB signal is too noisy to obtain reliable results, hence it is not considered anymore. The quality of the MAA signal is much better and consequently this data was used to fit the decay using a bi-exponential function. According to Figure 31, the ground state bleach seems to have similar dynamics as the MAA and thus the MAA lifetimes are assigned to the GSB as well. The obtained lifetimes are  $18 \pm 11$  ps for the fast and  $359 \pm 68$  ps for the long component. The induced monomer absorption could have a decay with two components as well. Due to the short lifetime of the first decay process and the high noise level in this region, only a mono-exponential fit can be assumed for sure and yields reliable and meaningful results. Consequently, the obtained lifetime of  $234 \pm 42$  ps might be the only lifetime or an average of both decay components.

	Rise time	Decay	
		Fast component	Long component
<b>GSB</b>	$\leq 150$ fs	$18 \pm 11$ ps	$359 \pm 68$ ps
<b>MAA</b>	$\leq 150$ fs	$18 \pm 11$ ps	$359 \pm 68$ ps
<b>IMA</b>	$\approx 400$ fs	?	$234 \pm 42$ ps

Table 1: Rise and decay times for thin terrylene films.

As a validation for the fitting results that were used to obtain the lifetimes and dynamics, the fitting parameters are compared with kinetic traces taken directly from the TA data. To obtain this traces, the intensity of the specific spectral feature is plotted against the pump-probe delay. To get meaningful results, the fit was used to discover the spectral position, where the TA signal is dominated by one of the portrayed features. For the modified aggregate absorption, this is the case at 3.3 eV, while the data for the induced monomer absorption is taken at 2.23 eV. The resulting curves are shown in Graph 32, compared with the traces obtained from the fit above. The fit results of both the modified aggregate absorption and the induced monomer absorption are in good agreement with the kinetic traces from the TA data. On the one hand, this again shows the high quality of the fitting procedure. It is able to properly reflect the TA data in the energetic domain, as seen in the spectra in Graph 29, as well as in the time domain, proved by the traces in Figure 32. On the other hand, as already stated above, it shows that the MAA and IA clearly have different dynamics, even if the fast component could be similar.

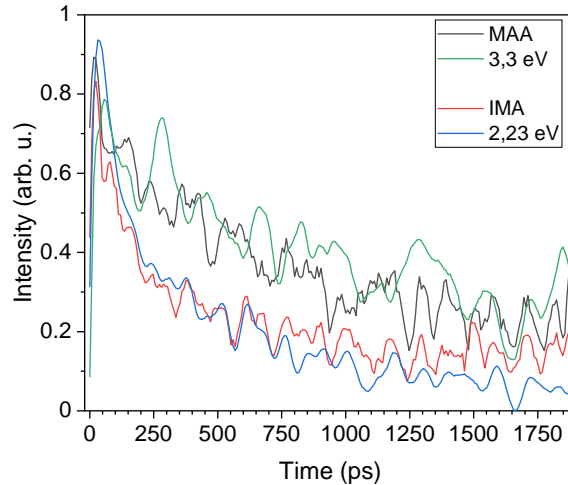


Figure 32: Comparison of dynamics obtained from fit parameters and directly from the TA data. All curves are smoothed and normalized for better visualization.

#### 4.4 Discussion of Electronic Dynamics in Thin Terrylene Films

In chapter 4.1, the properties of single molecules of terrylene in solution were investigated, revealing a simple to understand two-level system. Subsequently, the electronic properties of terrylene in the solid state were examined in this chapter. We found out, that the condensation leads to the change of numerous properties and the rise of new features. Time-dependent measurements were additionally used to reveal the dynamics behind those electronic processes. Compared to the monomers, thin films of terrylene show more complex dynamics, which are partially not fully understood yet. To use terrylene in future applications, for example in organic solar cells, it is especially important to understand the solid state properties and dynamics, to evaluate if terrylene can be used in such devices. In the following discussion, we want to summarize the obtained results. Even if we are not able to fully explain the electronic properties and processes yet, the collected results allow to point out conclusions and give the possibility for an interpretation of some of these observations. Moreover, this yields the schematic energetic level diagram shown in Figure 33.

Static absorption measurement shows that terrylene forms H-aggregates in the solid state, which are leading to a strong blueshift of the absorption band. Using transient absorption spectroscopy it was possible to discover other spectral processes, which occur on an ultrafast timescale. To fully understand the composition of the TA spectrum, a fitting procedure was established, which is capable of reflecting the whole spectrum in the energetic and temporal domain. This is especially remarkable, since the fit equation is only based on functions from the ground state measurements and five parameters for the relevant spectral regions.

Using this fit model for the transient absorption spectrum, it was shown that the signals in the spectral region between 3 and 4.6 eV are the result of an overlap between the ground state absorption spectrum of the H-aggregates and a 220 meV red-shifted, positive duplicate of this signal, which we called *modified aggregate absorption*. Since its differential absorbance signal is positive, it is only present after photoexcitation of the sample.

The second prominent feature occurs between 2.1 and 2.7 eV. As the modified aggregate absorption, this feature is only present in the excited sample, because it is a positive differential absorbance signal as well. Since it matches the spectral position and line shape of the ground state monomer response, it is assumed to be an absorption of induced monomer units. This is outstanding, since it shows the possibility to modify and break the aggregate on an ultrafast timescale.

Besides the investigation of the different spectral features which make up the TA spectrum, the fit allows to extract data about the temporal evolution of those features. By obtaining the kinetic traces for all spectral components, we were also able to determine the corresponding lifetimes. The GSB and MAA show almost the same dynamics, including an abrupt rise in under 150 fs, followed by a bi-exponential decay and an extremely long living component with a lifetime of

several nanoseconds. The lifetimes for the two decay components are  $18 \pm 11$  ps for the fast and  $359 \pm 68$  ps for the long component. The induced monomer absorption rises within 400 fs and thus is clearly delayed compared to the GSB and MAA. The IMA decays with a lifetime of  $234 \pm 42$  ps, again followed by an extremely long living component. It is now the goal to develop a deeper understanding about the the individual components and their coherences. For a better understanding of the following interpretation, Figure 33 shows an illustration of the electronic processes in thin terrylene films.

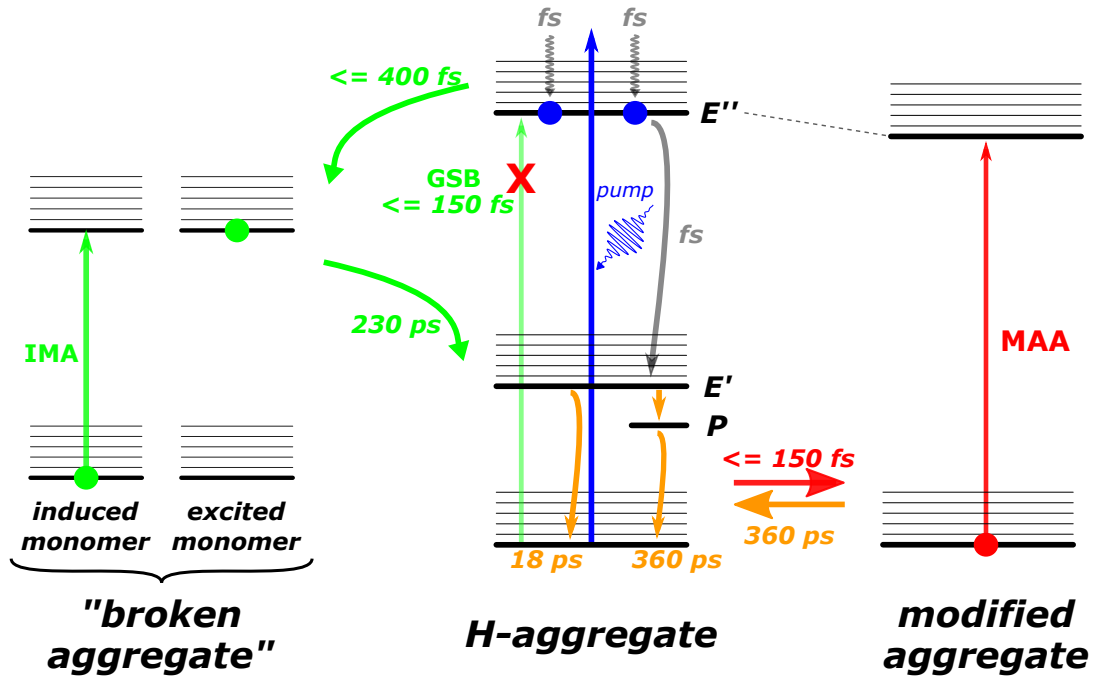
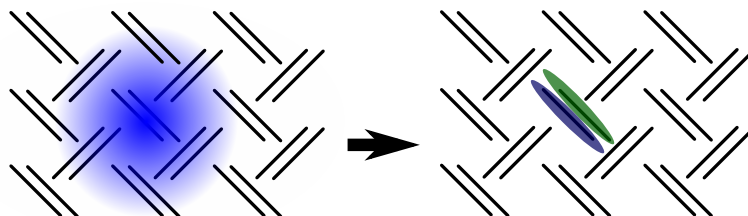


Figure 33: Illustration of the electronic processes in thin films of terrylene.

As a starting point, the great majority of terrylene molecules in the film form H-aggregates, as concluded from the static measurements. The ground state absorption spectrum of the films corresponds to the excitation of those dimers into the higher lying electronic state  $E''$ . The photoexcitation through the pump pulse leads to the depopulation of the ground state and thus a bleaching of the ground state absorption, which is observed as the GSB signal in the TA spectra. Since this happens immediately after the photoexcitation, the short rise time of under 150 fs, which is on the order of the time resolution, can be explained. The modified aggregate absorption has a positive TA signal and thus is a non-equilibrium signal. Because of this observation and because the MAA shows almost the same dynamics as the GSB, we conclude that it is associated to the depopulation of the aggregates ground state as well. Especially interesting is, that the MAA feature and the observed red-shift of 220 meV are also present within 150 fs and hence immediately after the excitation. This means that the shift is most likely of electronic origin, for example a fast structural reorganization or polarization of aggregate molecules as a response to the changed electronic environment after the ground state depopulation.

Another prominent feature is the absorption of induced monomers. To explain a possible origin of this feature, I want to point out two important observations. First, in the TA spectra the induced monomer absorption signal is positive, hence the formation happens in the highly excited sample. In apparent contrast to that, the observed absorption is coming from monomers in the ground state. We assume that the electrons in the highly excited sample recognize the possibility to reduce their energy by forming monomer units. In the H-aggregate, the excitation is delocalized at least across the dimer. Some unknown process, for example a structural change of the dimer which determines the formation time of 400 fs, could cause the localization of the excitation. This would result in a broken aggregate, consisting of an excited monomer and an induced monomer in the ground state, which is capable of explaining the monomer-like ground state absorption. This process is illustrated in Figure 34.



*Figure 34: Illustration of the delocalized excitation (left) and the collapse of the aggregate into an excited monomer (blue) and a monomer in the ground state (green) on the right side.*

Besides the formation of those features, their decay mechanisms are important as well. The amplitudes of the GSB and MAA are determined by the number of holes in the aggregate ground state. Consequently, explaining their decay requires to explain the re-population of this state. We found three distinct decay components, meaning that three different species are contributing to the relaxation. According to Kasha's theory of aggregates, the higher energy state  $E''$  will quickly relax to the lower energy state  $E'$ . We further assume, that the relaxation from the  $E'$  state to the ground state involves two species, on the one hand the direct transition from the  $E'$  state to the ground state with a lifetime of 18 ps and on the other hand an intermediate state  $P$ , which decays within 360 ps. Since the lifetime of the  $P$  state is significantly longer, it must be energetically stabilized, for example a species with strong polaronic character. Because we can only observe two lifetimes that are contributing to the ground state re-population, there are two possible relaxation pathways, which are shown in Figure 35. Either the re-population happens from the  $E'$  state with 18 ps and from the  $P$  state with 360 ps separately, or the  $P$  state is a reservoir for the  $E'$  state. In this case, the relaxation would still happen from the  $E'$  state within 18 ps, while the lifetime of 360 ps would correspond to an effective time constant for the  $E'$ - $P$ -equilibrium. Using only the time constants from the ground state re-population, these two relaxation pathways cannot be distinguished, since they result in the same rate equation for the re-population.

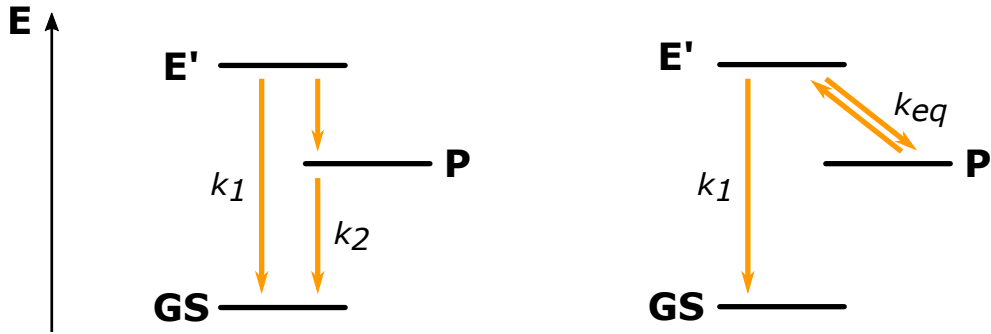


Figure 35: Two different relaxation pathways, which result in the same rate equation: Transitions from both states with different lifetimes  $k_1$  and  $k_2$  (left), and with the intermediate state  $P$  as a reservoir (right). The effective time constant for the equilibrium  $k_{eq}$  corresponds to the observed lifetime  $k_2$ .

The decay mechanism of the broken aggregate and the induced monomers are not that clear. We showed, that the decay of the induced monomer absorption is clearly different to the dynamics of the GSB and MAA. The obtained lifetime of 230 ps for the IMA means, that this lifetime corresponds to the disappearance of monomer units and consequently their recombination into aggregates. We are not able to explain the exact pathway of this relaxation, since the intensity of the IMA is noticeably lower than the intensities of GSB and MAA, so that possible contributions of the IMA to the ground state re-population are not observable.

Additionally to these most prominent features, the film perhaps has multiple other transitions and pathways, that cannot be discovered with the applied experimental techniques. For example the long living decay component, which is on the order of several nanoseconds and is seen in the decays of GSB, MAA and IMA. Most certainly, this results from trapped excitations, for instance at defects or grain boundaries.

## 5 Outro

New applications and developments in the optoelectronic field of research, like organic solar cells or organic light emitting diodes, require a strong understanding of the fundamental properties and the behavior of the different materials they consist of. In hybrid inorganic organic devices, organic semiconductors are mainly used because of their strong absorption and emission in the UV-vis range, as well as a high flexibility regarding their mechanical properties. The interaction with light and other materials, as well as the electric characteristics, are strongly depending on the electronic properties and dynamics in the material. In this thesis, the organic chromophore terrylene was investigated to determine and understand its electronic structure and transient properties to be able to evaluate if terrylene is a feasible candidate for HIOS applications and as a basis for future developments and research.

To obtain a fundamental understanding of the terrylene molecule it was examined as a single molecule in solution first. Static absorption and photoluminescence spectroscopy show that terrylene can be called a textbook-like molecule, showing strong absorption and photoluminescence in the visible range. Using time-correlated single photon counting it is possible to determine a lifetime of 4 ns for the excited state. Subsequently the transient absorption spectrum was fitted using a function that consists of the static spectra measured before. This fit model allows to consistently describe the TA data both in the energetic domain and temporal evolution. Accordingly, the different spectral features in the spectra can be assigned to physical processes and we are able to obtain their dynamics. In the terrylene molecule, all spectral processes show the same dynamics and thus are corresponding to the same excited state. Consequently, single molecules of terrylene are relatively simple systems. Both characteristics are promising for optoelectronic applications: the long-lived fluorescence in the visible region for example, is favorable for OLED's or display technology. The development of such complicated devices requires to understand the characteristics of the underlying materials as well as their interaction. Accordingly, molecules with simple electronic properties and comprehensible dynamics like terrylene are generally preferred.

In modern devices, organic semiconductors are most likely to be used in a solid state, rather than solvated. To understand how the condensation changes the electronic properties, thin films of terrylene were investigated next. A strong blueshift in the absorption, shifting the spectrum into the UV region, combined with a complete fluorescence quenching, suggests the formation of H-aggregates in the solid sample.

Compared to the solution, the transient absorption spectrum of the terrylene films is much more complex. A rather coarse fit model containing only five parameters and the monomer and film absorption spectrum, is able to reflect the complicated TA data for all pump-probe delays surprisingly well. Besides the ground state and excited state absorption of the aggregate, a monomer-like absorption feature, called *induced monomer absorption*, was found after

photoexciting the sample. This feature is especially notable, since it shows the possibility to break and modify aggregates and excite a monomer-like species on an ultra-fast time scale in the film. Additionally, the depopulation of the ground state gives rise to another absorption feature, which is a 220 meV red-shifted duplicate of the ground state absorption of the aggregates, which we called *modified aggregate absorption*.

The fact that the fit model is able to consistently describe the temporal evolution of all those features, it further allows the extraction of rise and decay times for all spectral features. Compared to the single molecule TA spectrum, the films show much more complex dynamics. The absorption of H-aggregates and modified aggregates rises almost instantaneously during 150 fs, i.e. on the order of the time resolution. Additionally, both features show the same dynamics, including a bi-exponential decay with a lifetime of 18 ps for the fast and 359 ps for the slow component, followed by an extremely long-living signal. Due to the same dynamics, we conclude that both features are associated to the depopulation of the ground state. As a result of this change in the electronic structure, a structural reorganization of the dimers could explain the observed redshift. The decay of both spectral processes involves two different species, most likely the lower energy state  $E'$  and a second, stabilized state  $P$ , which might be a polaronic state. As part of this thesis, the underlying decay process could not be resolved.

The induced monomer absorption rises delayed within 400 fs. We assume, that the above-resonance photoexcitation leads to small structural changes which determine the formation time, resulting in the localization of the excitation and thus the destruction of the dimer. This would give rise to an excited monomer and a monomer in the ground state, which is consequently responsible for the monomer-like absorption feature. The induced monomer absorption has an average lifetime of only 234 ps, until the monomer combine to form an aggregate again.

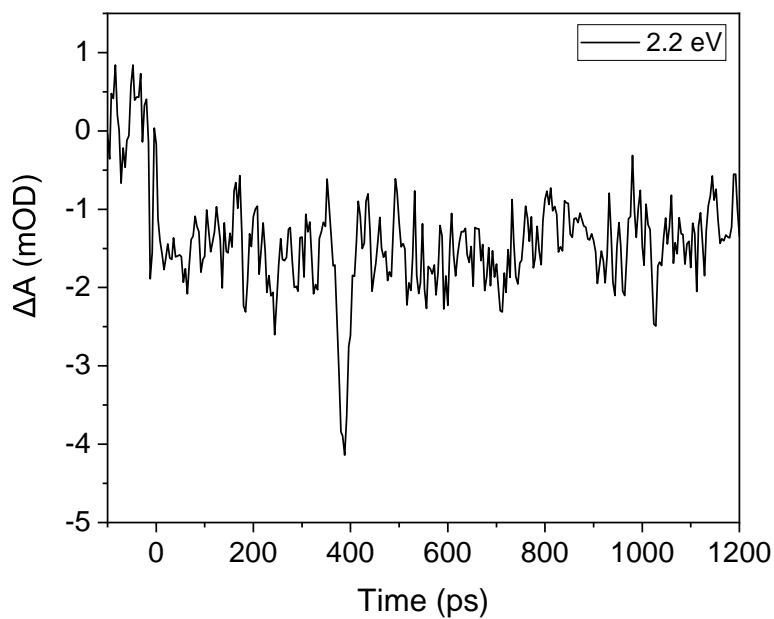
The possibility to modify the aggregates on an ultrafast timescale shows the great possibilities of organic semiconductors. While the aggregation leads to a shift of the absorption spectrum, the excitation of induced monomers allows to use the absorption wavelength of the monomer units as well. An important concept for hybrid inorganic organic devices is energy transfer between the different materials. For a variety of energy or charge transfer mechanisms, for example Förster resonance energy transfer, an overlap between the emission and absorption spectra of donor and acceptor is required. The ability to dynamically change the absorption spectrum and consequently the band gap in solid organic chromophores increases the flexibility and adaptability, for example to allow energy transfer to selected, adjacent materials. To further explore this possibility, the underlying mechanisms that lead to the formation and decomposition of such induced monomers need further investigation. As explained earlier, substituting organic chromophores allows to change and modify a variety of properties, which is one of their greatest advantages. That is why further work on this topic should determine, how substitution changes the properties and mechanisms of induced monomer absorption in H-aggregates.

## 6 References

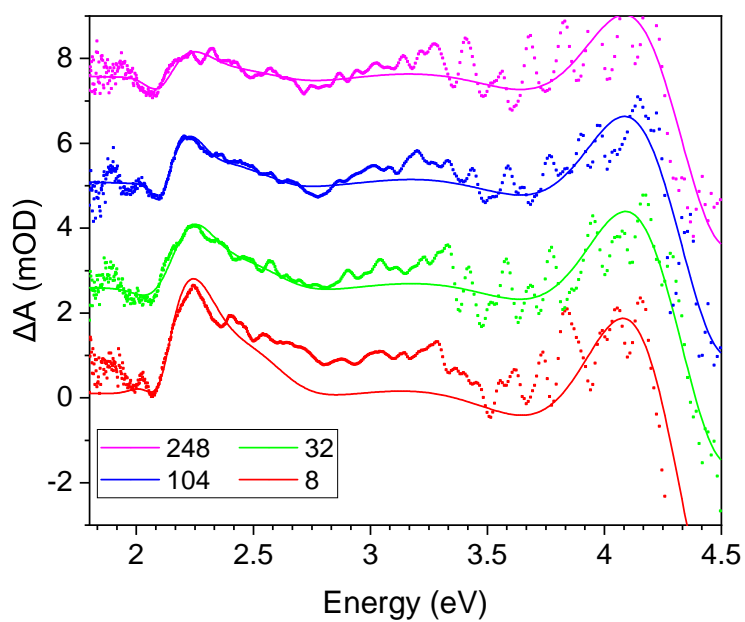
- [1] S. H. Mir, *et al.* *J. Electrochem. Soc.* **2018**, 165(8), 3137-3156.
- [2] X. Zhan, *et al.* *Adv. Mater.* **2011**, 23(2), 268-284.
- [3] A. M. Kelley. *Condensed-Phase Molecular Spectroscopy and Photophysics*, WILEY, 2012.
- [4] A. Köhler, H. Bässler. *Electronic Processes in Organic Semiconductors: An Introduction*. Wiley-VCH, 2015.
- [5] P. W. Atkins, J. de Paula. *Physikalische Chemie*. Wiley-VCH, 5th ed., 2010.
- [6] C. Jung, *et al.* *J. Am. Chem. Soc.* **2006**, 128(15), 5283-5291.
- [7] J. Clayden, N. Greeves, S. Warren. *Organic Chemistry*. Oxford, 2nd ed., 2012.
- [8] M. Kasha. *Radiation Research* **1963**, 20(1), 55-70.
- [9] N. J. Hestand, F. C. Spano. *Chem. Rev.* **2018**, 118(15), 7069-7163.
- [10] J. R. Lakowicz. *Principles of Fluorescence Spectroscopy*. Springer, 3rd ed., 2006.
- [11] K. E. Knowles, *et al.* *J. Mater. Chem. C* **2018**, 6, 11853-11867.
- [12] V. Gupta, Y. Ozaki. *Molecular and Laser Spectroscopy - Advances and Applications*. Elsevier, Volume 2, 2020.
- [13] S. A. Kovalenko, *et al.* *Phys. Rev. A* **1999**, 59(3), 2369-2384.
- [14] A. L. Dobryakov, *et al.* *Rev. Sci. Instrum.* **2010**, 81, 113106.
- [15] M. Quick, *et al.* *J. Phys. Chem. Lett.* **2016**, 7(20), 4047-4054.

## 7 Appendix

A.1: Intensity of the terrylene in para-xylene TA spectrum at 2.2 eV against the pump-probe delay.



A.2: Additional fit results for the TA film spectra.



## Selbstständigkeitserklärung

Ich erkläre hiermit, dass ich die vorliegende Arbeit selbstständig verfasst und noch nicht für andere Prüfungen eingereicht habe. Sämtliche Quellen einschließlich Internetquellen, die unverändert oder abgewandelt wiedergegeben werden, insbesondere Quellen für Texte, Grafiken, Tabellen und Bilder, sind als solche kenntlich gemacht. Mir ist bekannt, dass bei Verstößen gegen diese Grundsätze ein Verfahren wegen Täuschungsversuchs bzw. Täuschung eingeleitet wird.

---

Johannes Lütgert